Altered Elementary Calcium Release Events and Enhanced Calcium Release by Thymol in Rat Skeletal Muscle

Péter Szentesi,* Henrietta Szappanos,* Csaba Szegedi,* Monika Gönczi,† István Jona,* Julianna Cseri,* László Kovács,*† and László Csernoch*†

*Department of Physiology and †Cell Physiology Research Group of the Hungarian Academy of Sciences, Research Center for Molecular Medicine, Medical and Health Science Center, University of Debrecen, Debrecen, Hungary

ABSTRACT The effects of thymol on steps of excitation-contraction coupling were studied on fast-twitch muscles of rodents. Thymol was found to increase the depolarization-induced release of calcium from the sarcoplasmic reticulum, which could not be attributed to a decreased calcium-dependent inactivation of calcium release channels/ryanodine receptors or altered intramembrane charge movement, but rather to a more efficient coupling of depolarization to channel opening. Thymol increased ryanodine binding to heavy sarcoplasmic reticulum vesicles, with a half-activating concentration of 144 μM and a Hill coefficient of 1.89, and the open probability of the isolated and reconstituted ryanodine receptors, from 0.09 $\pm$ 0.03 to 0.22 $\pm$ 0.04 at 30 μM. At higher concentrations the drug induced long-lasting open events on a full conducting state. Elementary calcium release events imaged using laser scanning confocal microscopy in the line-scan mode were reduced in size, 0.92 $\pm$ 0.01 vs. 0.70 $\pm$ 0.01, but increased in duration, 56 $\pm$ 1 vs. 79 $\pm$ 1 ms, by 30 μM thymol, with an increase in the relative proportion of lone embers. Higher concentrations favored long events, resembling embers in control, with duration often exceeding 500 ms. These findings provide direct experimental evidence that the opening of a single release channel will generate an ember, rather than a spark, in mammalian skeletal muscle.

INTRODUCTION

Excitation-contraction coupling (E-C coupling) in skeletal muscle critically depends on the concerted action of two proteins, the dihydropyridine receptors (DHPRs) and ryanodine receptors (RyRs). The former, residing in the transverse-tubular (T-tubular) membrane, serves as the voltage sensor and can also carry the L-type calcium current (Ríos and Pizarro, 1991). The latter is the calcium release channel of the sarcoplasmic reticulum (SR) through which calcium ions enter the myoplasmic space upon stimulation (e.g., Meissner, 1994).

Spontaneous openings of RyRs in situ appear as elementary calcium release events in confocal images (Cheng et al., 1993). In mammalian muscle they can be subdivided into sparks and embers (Kirsch et al., 2001), the former resembling the *sparks* first described in heart (Cheng et al., 1993) and then in amphibian skeletal muscle (Tsugorka et al., 1995; Klein et al., 1996). *Embers*, a term introduced by González and co-workers (2000b) to denote events having long duration with constant fluorescence seem, on the other hand, to be more frequent in mammalian striated muscle as compared to sparks (Kirsch et al., 2001). Not only do mammalian calcium release events differ from those of frogs in their appearance, they seem to be affected less by classic drugs, e.g., caffeine, that influence E-C coupling and calcium sparks in amphibians (González et al., 2000a). Understanding this morphological variability and resistance to external influences should lead to a better understanding of how calcium release channels are regulated in mammalian striated muscle.

A wide range of phenol derivatives, including 4-chloro-meta-cresol (4CmC; Herrmann-Frank et al., 1996) and methyl *p*-hydroxybenzoate (Cavagna et al., 2000), were shown to alter RyR function. In a concentration of 0.2 mM and up, these substances increase the open probability of isolated RyRs and augment calcium release from intracellular calcium stores. It is interesting to note that a well known and widely used member of this group, thymol, has also been shown to alter calcium handling in a variety of cells, including skeletal muscle (Koshita and Oba, 1989; Kostyuk et al., 1991). In rabbit skeletal muscle, thymol first reduced the Ca^{2+}-ATPase activity, then increased the calcium permeability of the SR membrane. On neurons or on smooth muscle preparations, calcium transients could occur spontaneously in the presence of thymol, and the drug was found to increase the intracellular calcium concentration (Kostyuk et al., 1991; Hisayama and Takayanagi, 1986). Thymol is of special interest not only because it is widely used as a food preservative, but also because it is the stabilizer of liquid halothane, and its concentration might build up in the vaporizer during anesthesia. Despite its general use and definite actions on calcium homeostasis, no detailed analysis has so far been carried out to investigate the effects of thymol on E-C coupling in depth. Furthermore, no attempts were made to correlate the drug-induced alterations of SR calcium release and RyR function with the parameters of elementary calcium release events.

Here we show that thymol, at a concentration as low as 30 μM, enhances SR calcium release without major effects on the voltage sensor. Thymol is also shown to increase both

Submitted August 13, 2003, and accepted for publication October 21, 2003.

Address reprint requests to Dr. László Csernoch, Dept. of Physiology, University of Debrecen, PO Box 22, Debrecen H-4012, Hungary. Tel.: 36-52-416-634; Fax: 36-52-432-289; E-mail: csl@phys.dote.hu.

0006-3495/04/03/1436/18 $2.00

[^{3}H]ryanodine binding to heavy SR vesicles and the open probability (P_o) of the isolated and reconstituted RyRs through inducing long-lasting open events with full conductance at concentrations above 100 μM. These findings establish thymol as an ideal tool to study elementary calcium release events in mammalian muscle. Indeed, the drug altered the morphology of these events by increasing both their duration and the relative proportion of embers as compared to sparks. Higher concentrations of the drug induced extremely long embers that, in all likelihood, originate from a drug-modified channel, providing direct experimental evidence that embers, rather than sparks, represent the opening of a single RyR in mammalian skeletal muscle. Some of these results were presented to the Biophysical Society (Csernoch et al., 2002).

MATERIALS AND METHODS

Enzymatic isolation and voltage-clamping of single fibers

Single skeletal muscle fibers, isolated enzymatically from the *extensor digitorum communis* muscles of rats, were mounted into a double Vaseline-gap chamber as described earlier (Szentesi et al., 1997). In brief, rats of either sex were anesthetized and killed by cervical dislocation in accordance with the guidelines of the European Community (86/609/EEC) following a protocol approved by the institutional Animal Care Committee. The muscles were removed and were treated with collagenase (Type I, Sigma, St. Louis, MO) for 1–1.5 h at 37°C. After the dissociation, fibers were allowed to rest for at least 20 min.

The selected fiber was transferred into the recording chamber filled with relaxing solution (150 mM K-glutamate, 2 mM $MgCl_2$, 10 mM HEPES, and 1 mM EGTA). The fiber segments in the open-end pools were permeabilized using 0.01% saponin. Solutions were then exchanged to internal solution in the open-end pools (120 mM Cs-glutamate, 5.5 mM $MgCl_2$, 5 mM Na_2-ATP, 10 mM Na-phosphocreatine, 10 mM glucose, 5 mM HEPES, and 5 mM EGTA) and to external solution in the middle pool (140 mM tetraethylammonium-CH_3SO_3, 2 mM $CaCl_2$, 2 mM $MgCl_2$, 5 mM HEPES, 0.0003 mM tetrodotoxin, and 1 mM 3,4diamino-pyridine). All solutions were adjusted to pH 7.2 and 300 mosmol/l. The internal solution also contained 1 mM Antipyrylazo III (APIII) and 100 μM Fura-2 for the detection of $[Ca^{2+}]_i$. The length of the fiber segment in the middle pool was set to 500 μm.

The experimental setup and the data acquisition have been described in detail in our earlier reports (e.g., Csernoch et al., 1999b). The fiber was transilluminated using a tungsten halogen light source ($\lambda > 600$ nm) and was epiilluminated at 380 nm or at the isosbestic wavelength of Fura-2 using a 75-W Xenon arc lamp (Oriel 60000, Oriel Instruments, Stratford, CT). Light intensities were simultaneously recorded at 510, 720, and 850 nm for the detection of APIII absorbance and Fura-2 fluorescence. Fibers were voltage-clamped and the holding potential was set to −100 mV. All experiments were performed at 16–18°C.

Preparation of SR vesicles and RyRs

Heavy SR (HSR) vesicles were isolated from either rabbit or rat skeletal muscle as described earlier (Szegedi et al., 1999, and Csernoch et al., 1999b, respectively). Rabbit HSR vesicles were used for ryanodine binding experiments, whereas the ryanodine receptor calcium release channel was isolated from rat HSR vesicles. In brief, skeletal muscles were removed from the *longissimus dorsii* (rabbit) or from the front and hind legs of those rats that were used in the Vaseline-gap experiments. The muscles were cut into small pieces, quickly frozen using liquid nitrogen, and stored at −70°C until further use. Vesicles were obtained by first homogenizing the tissue then removing the unsolubilized particles in a clinical centrifuge. Crude membrane fraction was collected from the supernatant by centrifugation at 40,000 × g (30 min). The actomyosin content of the pellet was then dissolved in 600 mM KCl and the crude microsome fraction was collected by centrifugation at 109,000 × g (30 min). The microsome was loaded onto a 20–45% linear sucrose gradient and spun for 16 h at 90,000 × g (4°C) in a swingout (SW-27) Beckman rotor (Beckman-Coulter, Fullerton, CA). The protein-ring corresponding to the HSR fraction was extracted from the 36–38% region. Vesicles were collected at 124,000 × g for 60 min then resuspended in 92.5 mM KCl and 18.5 mM K-MOPS at pH = 7.0 for vesicular measurements or in 0.4 M sucrose and 10 mM K-PIPES at pH = 7.2 for RyR preparation. Samples were stored at −70°C until further use.

For preparation of RyR, the rat HSR vesicles (3 mg/ml) were solubilized for 2 h at 4°C with 1% CHAPS (3[(3-chloramidopropyl)dimethyl-amino]-1-propanesulfonate) in a solution containing 1 M NaCl, 100 μM EGTA, 150 μM $CaCl_2$, 5 mM AMP, 0.45% phosphatidylcholine, 20 mM Na-PIPES at pH = 7.2, and protease inhibitors (Csernoch et al., 1999b). Unsolubilized proteins were removed by centrifugation at 59,000 × g, and subsequently the supernatant was layered on top of a 10–28% sucrose gradient also containing 1% CHAPS, 0.7 M NaCl, 10 mM AMP, 0.5% phosphatidylcholine, 70 μM EGTA, 100 μM $CaCl_2$, 1 mM DTT (dithiothreitol), and 13 mM Na-PIPES at pH = 7.2. Solubilized SR membranes were centrifuged through the sucrose gradient for 16 h at 90,000 × g (4°C) in a swingout (SW-27) Beckman rotor. Fractions containing RyRs were collected in small aliquots. They were then rapidly frozen in liquid nitrogen and stored at −70°C.

Calculation of $[Ca^{2+}]_i$ and R_{rel}

In Vaseline-gap experiments the changes in myoplasmic free calcium concentration ($[Ca^{2+}]_i$) were calculated from APIII absorbance with the correction for intrinsic fiber absorbance at 850 nm and from Fura-2 fluorescence using the kinetic correction. Resting, as well as small changes in $[Ca^{2+}]_i$ were determined from changes in Fura-2 saturation, whereas large increases in $[Ca^{2+}]_i$ were determined from changes in APIII absorbance.

The rate of calcium release from the SR (R_{rel}) was calculated from the calcium transients using the procedure described in Szentesi et al. (1997). In brief, four parameters of the removal model were fitted simultaneously, $k_{off,M-P}$ (Mg^{2+} off rate from parvalbumin), PV_{max} (maximal transport rate of SR calcium pump), and $k_{off,Ca-E}$ and $k_{on,Ca-E}$ (the rate constants of calcium binding to EGTA). The calculated R_{rel} records were corrected for the depletion of calcium in the SR and expressed as a percentage of SR content. The voltage dependence (V_m) of either component of calcium release, $R_{rel,i}(V_m)$, where i = peak or steady level, was assessed by fitting the two-state Boltzmann function

$$R_{rel,i}(V_m) = R_{rel,i}[max]/(1 + \exp\{-(V_m - V_{50})/k\}), \quad (1)$$

where $R_{rel,i}[max]$ is the maximal release rate, V_{50} is the voltage at half-maximal release rate, and k is the slope factor, to the calculated data.

Intramembrane charge movement

Intramembrane charge transfer was calculated by measuring membrane currents in response to depolarizing and hyperpolarizing pulses as described in detail previously (Szentesi et al., 1997). Briefly, the linear capacitive current was determined from hyperpolarizing pulses of −20 mV in amplitude. This current was then scaled and subtracted from those measured during depolarizing steps. The nonlinear capacitive current, representing intramembranous charge transfer, was integrated to give the amount of charge moved during the pulse (Q). To assess the membrane potential dependence of charge transfer, $Q(V_m)$, the measured charge was fitted with the Boltzmann function

$$Q(V_m) = Q_{max}/(1 + \exp\{-(V_m - V_{50})/k\}), \quad (2)$$

where Q_{max} is the maximal available charge, and V_{50} and k have their usual meaning.

Ryanodine binding

Ryanodine binding assay was carried out using [^{3}H]ryanodine in an incubation medium of 1 M NaCl, 25 mM Na-PIPES at pH 7.1, 1 mM Pefabloc, (Fluka, Buchs, Switzerland), 300 μM $CaCl_2$, and 205 μM EGTA. 50 μl aliquots, containing 25 μg protein were incubated at 37°C for 2 h, with the various concentrations of the radioligand and of thymol (Herrmann-Frank et al., 1996). The reaction was terminated by immediately filtering the samples on a Bio-Dot 96 well filter apparatus (Bio-RAD Lab., Hercules, CA) using Millipore-50 filter paper (Millipore, Billerica, MA). The dots were than rinsed with equal aliquots of washing medium without ryanodine (hot and cold), that were otherwise identical to the incubation medium. Filter papers were cut into appropriate pieces and their radioactivity was determined using a liquid scintillation counter. Nonspecific binding was determined in the presence of 50–100 μM ryanodine, added to the incubation mixture before the radioligand. Thymol was found not to affect the nonspecific binding. Binding data, as well as the concentration-dependent effects of thymol on binding, were fitted using the Hill equation

$$B/B_{max} = [X]^n/([EC_{50}]^n + [X]^n), \quad (3)$$

where B is the concentration of the bound form, B_{max} is the theoretical maximum of B, X is the ligand in question (ryanodine or thymol), and n is the Hill coefficient. Experiments were carried out in quadruplets and the averaged data were used in the calculations.

Planar lipid bilayer measurements

CHAPS-solubilized ryanodine receptors (Tripathy and Meissner, 1996) were incorporated into planar lipid bilayers formed across a 200-μm aperture of a nolrene cup using a lipid mixture composed of phosphatidylethanolamine, phosphatidylserine, and phosphatidylcholine in the weight ratio of 5:4:1. Lipids were dissolved in *n*-decane up to a final concentration of 20 mg/ml as described in our previous reports (e.g., Csernoch et al., 1999b). Reconstitution was initiated in symmetric buffer solution (250 mM KCl, 100 μM EGTA, 150 μM $CaCl_2$, and 20 mM PIPES, at pH 7.2), by adding a small aliquot of the solubilized receptor to the *cis* (cytoplasmic) side. The current signal was filtered at 1 kHz through an eight-pole low-pass Bessel filter and digitized at 6 kHz using an Axopatch 200 amplifier and pClamp software (Axon Instruments, Foster City, CA). Channels with conductance >400 pS were accepted as RyRs. Open probability values were calculated from 1-min-long segments of the current traces. Measurements were carried out at 22–25°C, and thymol was applied in the *cis* chamber.

Measurement of calcium sparks

Single fibers, isolated as detailed above, were mounted into a chamber with glass bottom. Cells were treated with a modified relaxing solution (125 mM K-glutamate, 10 mM HEPES, 1 mM EGTA, 6 mM $MgCl_2$, 5 mM Na_2-ATP, 10 mM Na-phosphocreatine, 10 mM glucose, 0.13 mM $CaCl_2$, and 8% dextran) containing 0.002% saponin for 2–3 min. Permeabilization of the surface membrane was monitored by the addition of 50 μM fluo-3 into the solution and imaging of the fiber. This solution was then exchanged to a K_2SO_4-based internal solution (95 mM K_2SO_4, 10 mM HEPES, 1 mM EGTA, 6 mM $MgCl_2$, 5 mM Na_2-ATP, 10 mM Na-phosphocreatine, 10 mM glucose, 0.13 mM $CaCl_2$, 0.1 mM fluo-3, and 8% dextran) since the presence of sulfate was shown to increase the spark frequency without affecting the spark morphology in mammalian preparations (Csernoch et al., 2003; Zhou et al., 2003).

Fibers were imaged using an LSM 510 laser scanning confocal microscope (Zeiss, Oberkochen, Germany). Line-scan images ([x,t]) were taken at 1.54 ms/line and 512 pixels/line (pixel size 0.142 μm) with a 40× water immersion objective (1.2 NA; Zeiss) parallel to the fiber axis. Fluo-3 was excited with an argon ion laser (at 488 nm; 5% laser intensity), and emitted light was collected through a bandpath filter and digitized at 12 bits. Any bleaching of the dye was corrected for. To avoid photodamage, the same position was not imaged twice. The bleaching-corrected images (F[x,t]) were then normalized to baseline fluorescence (F_0[x]).

Elementary calcium release events were captured using an automatic computer detection method based on those described earlier (e.g., Cheng et al., 1999). In brief, the program identified elementary events as regions with fluorescence above a relative threshold, calculated from the noise in the images, and having amplitudes >0.3 $\Delta F/F_0$ units. The eventless portion of the image was used to calculate bleaching (averaged over the x axis and smoothed) and F_0[x] (averaged, but not smoothed over the t axis). The program also determined the parameters of the identified events: amplitude (as $\Delta F/F_0$); spatial half-width measured at the time of the peak (full width at half-maximum, FWHM); duration; and rise time for sparks and sparks with embers. For the lone embers, the average amplitude, duration, and FWHM parameters were determined. FWHM was obtained from fitting a Gaussian function to the spatial distribution obtained by averaging three lines at the peak for sparks or by all lines except the first and last 10 ms of the event for lone embers.

Chemicals and statistics

Fura-2 and Fluo-3 were purchased from Molecular Probes (Eugene, OR), whereas APIII was purchased from ICN Biomedicals (Aurora, OH). Protease inhibitors were from Boehringer (Mannheim, Germany), from Merck (Darmstadt, Germany), and from Sigma (St. Louis, MO). Lipids were obtained from Avanti Polar Lipids (Alabaster, AL), [^{3}H]ryanodine was from Dupont (Boston, MA), and all other chemicals were from Sigma. Thymol was prepared as a stock of 300 mM in DMSO.

In statistical analyses all values were expressed as mean ± SE. Statistical significance was calculated with Student's t-test assuming significance for $p < 0.05$.

RESULTS

Thymol has modest effects on intramembrane charge movement

Recent reports demonstrated the suppression of L-type calcium currents by thymol on cardiac (Magyar et al., 2002) as well as skeletal (Szentandrássy et al., 2003) muscle cells with half-inhibitory concentration above 100 μM. To understand the effects of the drug on E-C coupling we first tested the involvement of the voltage sensor as a putative binding site of thymol. Intramembrane charge movements were thus measured on rat skeletal muscle fibers mounted into the double Vaseline-gap chamber.

Fig. 1 *A* presents nonlinear capacitive currents in the absence and presence of the drug. The transients were recorded in response to 100-ms-long depolarizing pulses exploring the −80–0 mV voltage range. The actual intramembrane charge movement currents were normalized to fiber capacitance to take into account the differences in fiber size or any possible change in passive electrical properties during the experiments. It should be noted, however, that the linear capacitance, on average, did not change significantly

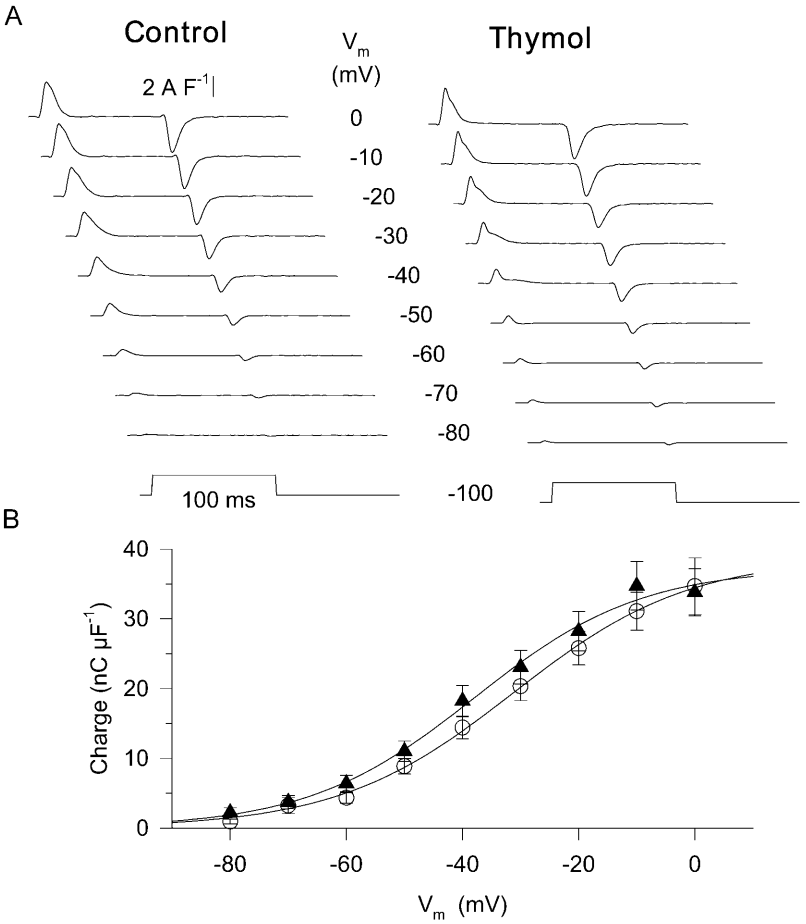

FIGURE 1 The effect of thymol on intramembrane charge movement. (*A*) Nonlinear capacitive currents in the absence and presence of 300 μM thymol. The holding potential was set to −100 mV and the currents representing the intramembrane charge displacement were recorded in response to 100-ms-long depolarizing pulses. The membrane potentials during the pulses are given in each row. The current traces were normalized to the linear capacitance (10.5 nC) of the fiber. (*B*) The Boltzmann distribution of intramembrane charge. The current records presented in *A* and six other fibers were integrated and the calculated charges at corresponding voltages were averaged. Eq. 1 was fitted to the data points to assess the voltage dependence of charge displacement. Superimposed curves were generated using the parameters obtained from the fits (Q_{max} = 38.8 and 37.4 nC μF^{-1}; V_{50} = −31.2 and −38.0 mV; k = 15.1; and 14.4 mV in control (○) and in thymol (▲), respectively).

during the course of these experiments since it was found to be 11.3 ± 1.1 nF (n = 7) under control conditions and 9.4 ± 1.7 nF on the same cells after the addition of 300 μM thymol.

To assess the voltage dependence of charge transfer, the currents were integrated and Eq. 2 was fitted to the charge versus voltage data both before and after the addition of thymol. Average values of the parameters from these fits are presented in Table 1. To visualize the effects of thymol on the voltage dependence of charge transfer, Fig. 1 *B* plots the charge as a function of membrane potential during the test pulse. Thymol, at the concentration tested, shifted the voltage dependence to the left along the voltage axis, by 10 mV, together with a slight decrease in Q_{max} (the maximally available charge). Whereas the changes in V_{50} were statistically significant, the changes in Q_{max} and in the steepness remained, on average, within the limits of statistical variation. As it will be detailed below, thymol already had significant effects on SR calcium release at a concentration of 30 μM. Table 1, therefore, presents average values for the voltage dependence of charge movement at this concentration.

These data, on the one hand, establish that the suppression of L-type calcium currents seen in earlier studies with phenol analogs (Fusi et al., 2001) or with thymol itself cannot be accounted for by an effect on the voltage sensor. Furthermore, the slight shift in the voltage dependence of intramembrane charge movement could also not explain its effects on previously reported effects on calcium handling.

Thymol increases the calcium transients

Fig. 2 illustrates the effect of extracellular application of 30 μM thymol on the calcium transients elicited by 60–100-ms-long depolarizing pulses under voltage-clamp conditions. Fig. 2 *A* shows a series of calcium transients, measured with APIII, elicited by depolarizing pulses of various lengths from −40 to 0 mV. Measurements in thymol were taken 5−10 min after the solution exchange. This was believed to be long enough for the drug to reach its binding site and exert its full effect. Application of thymol produced an ~50% increase in the maximal amplitude of the calcium transient from 1.5 ± 0.3 to 2.2 ± 0.4 μM (n = 9). The transients showed a continuous increase in control and after the addition of 30 μM thymol. The increase was present both in the rate of rise and in the amplitude of the calcium signals. Fig. 2 *B* shows the voltage dependence of the mean (n = 9) maximum change in $[Ca^{2+}]_i$ reached in control conditions (*open symbols*), and upon thymol application (*solid symbols*). In

TABLE 1 Effect of thymol on intramembrane charge movement

	Q_{max} (nC μF^{-1})	V_{50} (mV)	k (mV)
Control ($n = 7$)	35.2 ± 3.1	−25.9 ± 2.6	12.0 ± 1.5
30 μM thymol	34.0 ± 4.4	−34.8 ± 2.7*	11.6 ± 0.9
Control ($n = 8$)	35.4 ± 2.7	−27.8 ± 2.4	11.4 ± 1.2
300 μM thymol	35.8 ± 3.8	−39.8 ± 2.9*	13.7 ± 0.6

Parameter values obtained by fitting Eq. 2 to the voltage dependence of intramembrane charge movement.
*Significant difference from control.

average, the drug produced a 58% elevation of the peak calcium transient. This effect of thymol was associated with a slight, but not significant, change in resting $[Ca^{2+}]_i$, which, within this series of measurements, exhibited a mean value of 51 ± 6 and 72 ± 9 nM before and after addition of the drug.

SR permeability is augmented by thymol

Fig. 3 presents the rate of calcium release from the SR (R_{rel}; see Methods) calculated from calcium transients shown in Fig. 2. The figure demonstrates that the above-mentioned effects of thymol on $[Ca^{2+}]_i$ were present on R_{rel} at every membrane potential tested. Thymol increased both the early peak and the sustained steady level of the calcium release. On average the maximal increase in the peak in 30 μM thymol was found to be 28.4 ± 4.0 μM ms^{-1} ($n = 10$) for a 100-ms-long depolarization to 0 mV as compared to 17.8 ± 2.2 μM ms^{-1} measured on the same fibers under control conditions. Whereas the maximal increase in the steady level was found to be 10.6 ± 2.0 μM ms^{-1} ($n = 10$) in the presence of the drug and 7.3 ± 1.0 μM ms^{-1} was measured on the same fibers under control conditions, the effect of thymol was reversible. After washout, the peak returned to

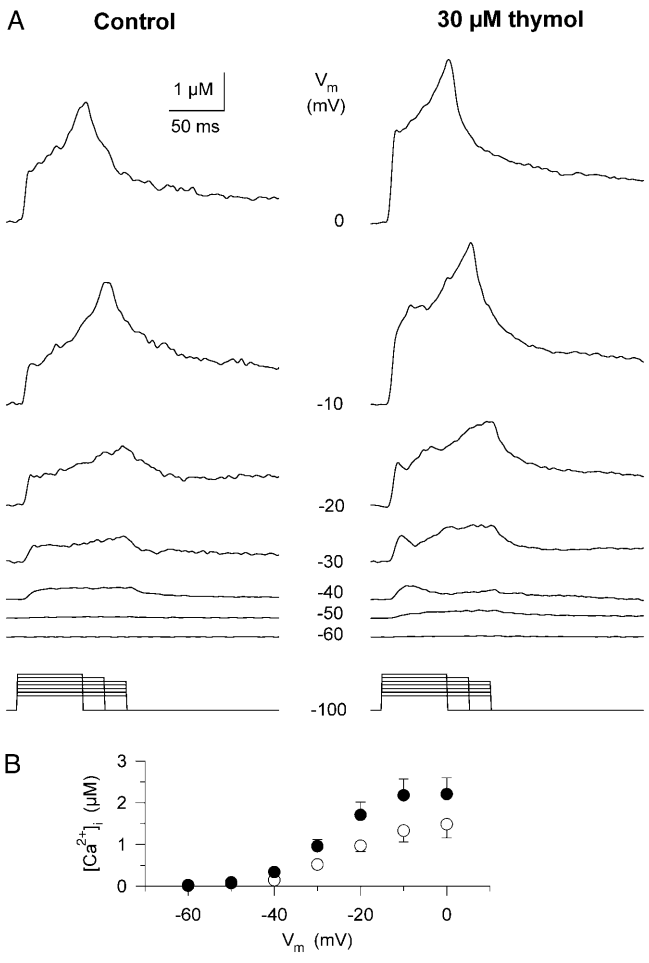

FIGURE 2 Effect of 30 μM thymol on the calcium transients. (*A*) Changes in $[Ca^{2+}]_i$ measured with APIII before and after the addition of the drug. The holding potential was set to −100 mV and the fiber was then depolarized to the indicated voltages for 60–100 ms. [APIII] = 680–1380 μM. (*B*) The maximal increase in $[Ca^{2+}]_i$ during the calcium transients was averaged from 10 fibers and plotted as a function of the membrane potential during the depolarizing pulses.

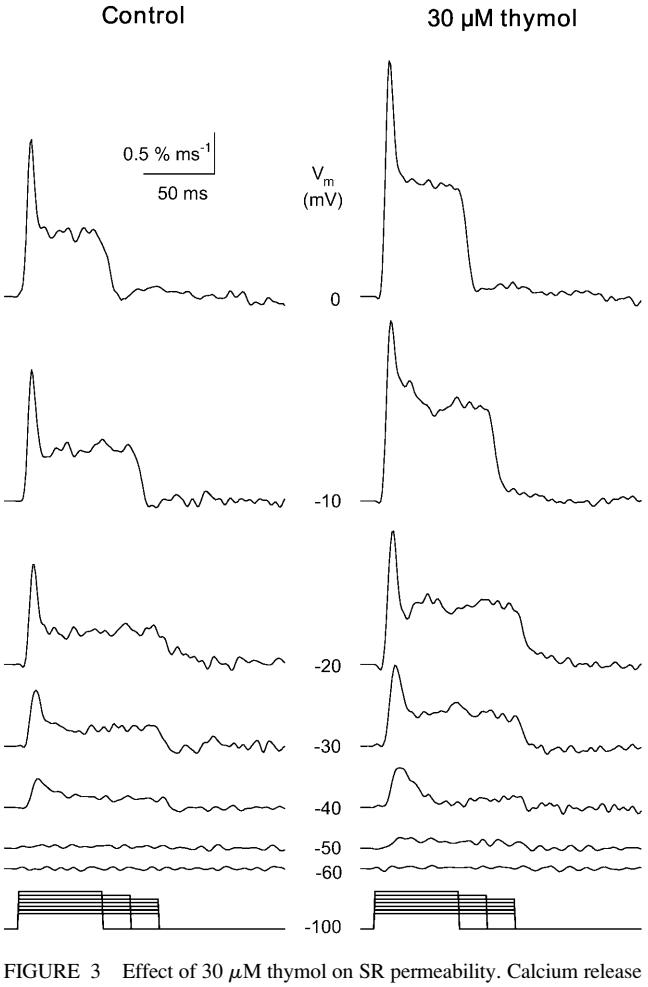

FIGURE 3 Effect of 30 μM thymol on SR permeability. Calcium release from the SR was calculated from the transients presented in Fig. 2 and then corrected for the depletion of calcium in the SR. The parameters of the removal model used in the calculation of SR calcium release were $k_{off,Mg-P} = 9.4$ s^{-1}, $PV_{max} = 2.4$ mM s^{-1}, $k_{on,Ca-E} = 0.76$ μM^{-1} s^{-1}, and $k_{off,Ca-E} = 6.3$ s^{-1}. SR calcium content, 2.0 mM, was determined from the transient obtained in response to the depolarization to 0 mV in control, and used throughout.

82 ± 9% whereas the steady level returned to 82 ± 6% of the control level.

To describe the effect of thymol on the calcium release process the rate of calcium release was corrected for depletion of calcium in the SR and the obtained transients were normalized to SR contents. This content was found to be fairly stable over the fibers included into the present study (1.7 ± 0.2 mM; $n = 10$) and to be unaltered by the treatment with 30 μM thymol. All calculation used, therefore, the same SR content in a given fiber in the absence and presence of the drug. Similarly, thymol left the parameters of the removal model essentially unaltered. The corresponding values of the parameters, if fitted independently in control and in the presence of the drug, were $k_{off,M-P} = 7.4 \pm 1.3$ and $4.5 \pm 0.7\ s^{-1}$; $PV_{max} = 2.5 \pm 0.6$ and $2.2 \pm 0.4\ mM\ s^{-1}$; $k_{off,C-E} = 7.2 \pm 1.4$ and $6.0 \pm 0.8\ s^{-1}$; and $k_{on,C-E} = 1.4 \pm 0.3$ and $2.2 \pm 0.9\ \mu M\ s^{-1}$.

The effect of thymol on calcium release is presented in Fig. 4, where pooled data of the two kinetic components of SR permeability are shown as a function of membrane potential in control, in the presence of the drug and after wash. The individual data points were normalized before averaging. To this end Eq. 1 was fitted to the data—peak or steady level versus voltage—in control for each and every fiber and the obtained maximum ($R_{rel,i}[max]$ in Eq. 1) was used for normalization. Fig. 4 reveals an elevation of both the early peak and the steady component of SR permeability reaching >50% in 30 μM thymol. It also shows that significant recovery was achieved after the removal of the drug.

To quantify the increase caused by the drug, Eq. 1 was fitted to the data—peak or steady level versus voltage—in the presence and absence of thymol and after wash in every fiber. The obtained parameters, P_{max} or Sl_{max} ($R_{rel,i}[max]$ in Eq. 1 with i = peak or steady level, respectively), the midpoint voltage, and the slope factor, are presented in Table 2, after averaging. The data reveal that 30 μM thymol significantly ($p < 0.05$) elevated the early peak and the steady level, although the effect on the steady level was somewhat smaller than on the peak (51 ± 17 vs. 62 ± 17%).

Comparing the voltage dependence of the different components as well as the effect of thymol on the voltage dependence did not reveal any systematic difference or trend. The fact that thymol had very little effect on the voltage dependence of either component suggested a voltage-independent activation of SR permeability by the drug.

These data establish that thymol elevates SR permeability in a voltage-independent manner. The extent of elevation is equal for the two kinetic components, peak and steady level, of SR permeability.

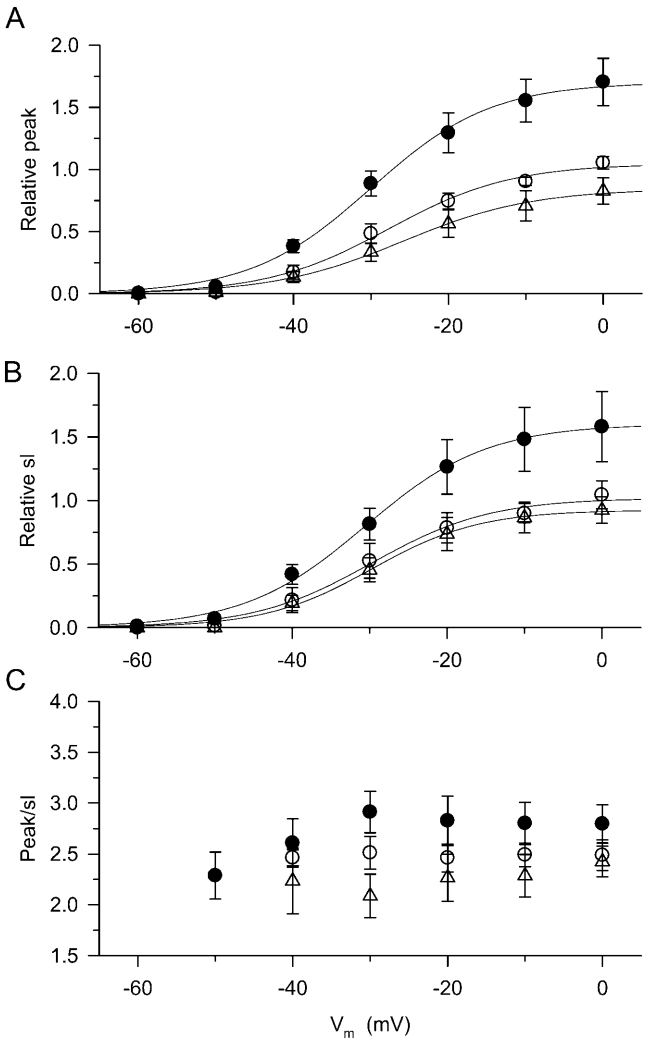

FIGURE 4 Effects of thymol on the kinetic components of SR permeability. (*A*) Voltage dependence of the peak component of SR permeability. The voltage dependence of the peak of SR permeability was first fitted with Eq. 1 in control. The obtained maximum was used to normalize all values in the given fiber both before (○) and after the addition (●), and after the removal of the drug (△). The normalized values from 10 fibers were averaged before plotting them. Superimposed curves present the least-squares fit of Eq. 1 with $Max = 1.05 \pm 0.04$, 1.70 ± 0.04, and 0.84 ± 0.03; $V_{50} = -27.7 \pm 1.2$, -29.9 ± 0.8, and -25.9 ± 1.0 mV; and $k = 7.9 \pm 0.9$, 7.8 ± 0.6, and 8.4 ± 0.7 mV in control, in the presence of thymol, and after wash. (*B*) Voltage dependence of the steady component of SR permeability. The steady level for a given transient was calculated as the average of the last 20 points during the depolarizing pulse. The values were then normalized and averaged as described in *A*. Superimposed curves again represent the fit of Eq. 1 with $Max = 1.02 \pm 0.04$, 1.70 ± 0.03, and 0.93 ± 0.02; $V_{50} = -29.7 \pm 1.2$, -30.5 ± 0.7, and -29.7 ± 0.7 mV; and $k = 7.6 \pm 0.9$, 7.9 ± 0.5, and 6.9 ± 0.6 mV in control, in the presence of thymol, and after wash. (*C*) Voltage dependence of the peak/steady ratio. At voltages <-40 mV, with the exception of data in thymol at -50 mV, the values were too small to allow a reliable determination of the ratio.

Inactivation of R_{rel} is unaffected by thymol

Previous sections have demonstrated that thymol enhances the permeability of the SR membrane when stimulated through the voltage sensors. This augmentation could, in general, occur through increased activation, decreased inactivation, or both. In the following we tested whether

TABLE 2 Voltage dependence of SR calcium permeability

	Peak			Steady level		
	Max* (μM ms^{-1})	V_{50} (mV)	k (mV)	Max* (μM ms^{-1})	V_{50} (mV)	k (mV)
Control ($n = 10$)	16.9 ± 1.9	−28.5 ± 2.3	6.5 ± 0.5	6.2 ± 0.8	−28.7 ± 2.6	6.4 ± 0.7
30 μM thymol	25.6 ± 3.1†	−31.0 ± 1.2	7.0 ± 0.5	8.6 ± 0.9†	−31.5 ± 1.0	7.6 ± 0.5
Wash	13.3 ± 1.6	−22.8 ± 3.5	8.6 ± 0.9†	5.2 ± 0.5	−26.7 ± 2.3	7.4 ± 0.5

Parameter values obtained by fitting Eq. 1 to the voltage dependence of SR permeability. Values represent mean ± SE.
*Denoted as $R_{rel,i}[max]$ with i = peak or steady level in Eq. 1.
†Significant difference from control.

the drug alters the inactivation of the calcium release channels.

To study the calcium-dependent inactivation of calcium release, double pulses, separated by 10-ms-long repolarization to −120 mV to facilitate the return of intramembranous charge to its resting state, were applied with varying the amplitude of the first (pre-) pulse and keeping the second (test) constant. The increase in $[Ca^{2+}]_i$ during the prepulse caused a marked suppression of the peak during the test pulse (Simon et al., 1991; Szentesi et al., 2000) which corresponded to the inactivation of the channels. Fig. 5 presents SR permeability elicited by double pulses in the absence (*left panel*) and in the presence of 30 μM thymol (*right panel*). The steady-state inactivation was assessed as the relative suppression of the inactivating component (peak minus steady level = P–Sl) during the test pulse (Szentesi et al., 2000), which was the largest when no prepulse was applied (P_0–Sl_0). The effect of a prepulse, if it elicited measurable calcium release, was to suppress the inactivating component of the subsequent test pulse (P_1–Sl_1) without affecting the steady level. The figure shows that 30 μM thymol did not cause any visible change in how the channels inactivate, although it enhanced calcium release both during the prepulse and the test pulse.

Previous studies revealed that the relative suppression—the inactivating component of a conditioned test pulse that is normalized to the inactivating component of a non-conditioned test pulse, (P_1–Sl_1)/(P_0–Sl_0)—is a good measure of channel inactivation (Pizarro et al., 1997). Fig. 6 *A* thus presents the relative suppression as a function of the maximal SR calcium release during the prepulse in control and in the presence of 30 μM thymol. In control the relationship is linear as shown previously (Pizarro et al., 1997; Szentesi et al., 2000). It describes a direct link between the calcium concentration reached in the triad and the number of channels that were inactivated during the test pulse. In the presence of thymol the linear relationship was maintained although, due to the larger release in the presence of the drug, it was shifted to the right. Furthermore, if the data were normalized to the maximum release on the given fiber in control and in thymol, respectively, the linear functions were identical in the absence and the presence of the drug (Fig. 6 *B*).

By plotting the absolute suppression, $\Delta(P$–$Sl) = (P_0$–$Sl_0) - (P_1$–$Sl_1)$, as a function of the inactivating component of the prepulse from different fibers (Fig. 6, *open symbols* in control, *solid symbols* in thymol), the relationship became independent of V_{test}, resembling a straight line (Fig. 6 *C*). Fitting straight lines to the data, independently to the values in control and in the presence of the drug, gave regression coefficients close to unity suggesting that exactly those channels were lost from the test pulse that were inactivated

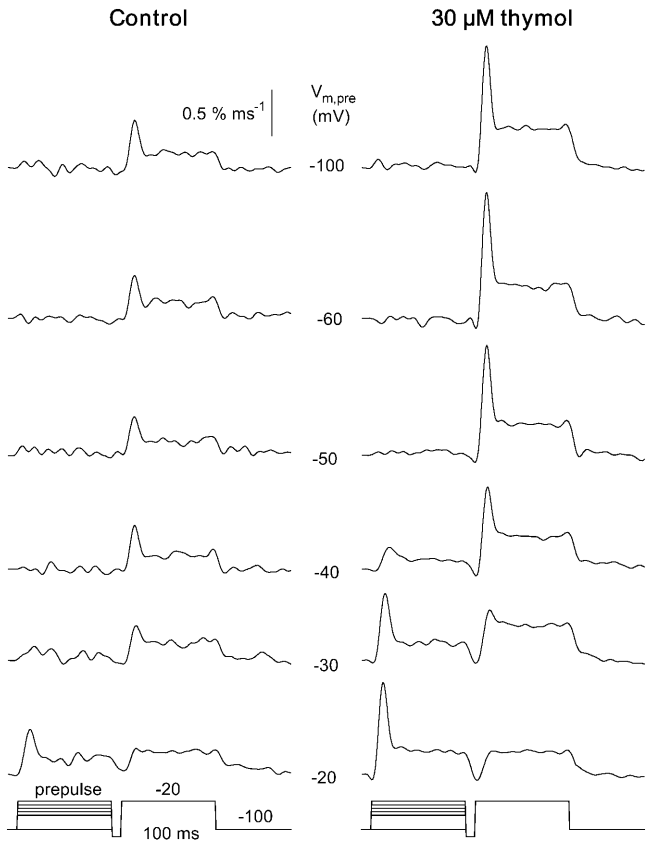

FIGURE 5 Inactivation of SR calcium release in the presence of thymol. SR permeability was measured with double pulses. The test pulse was always a depolarization to −20 mV, whereas the membrane potential during the prepulse was varied between −100 mV, the holding potential, and −20 mV (values indicated between the traces). The depletion factor, 2.0 mM, was determined in control and used throughout the experiment. The parameters of the removal model were $k_{off,Mg–P} = 16.0\ s^{-1}$, $PV_{max} = 1.6$ mM s^{-1}, $k_{on,Ca–E} = 0.51\ \mu M^{-1}\ s^{-1}$, and $k_{off,Ca–E} = 3.0\ s^{-1}$.

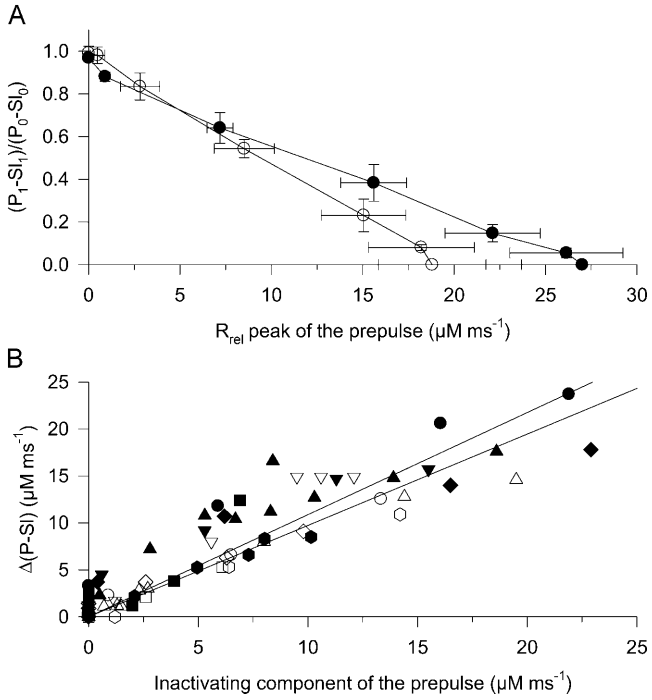

FIGURE 6 Suppression of the inactivating component of SR permeability. The inactivating component was calculated as the difference between the peak (P) and the steady level (Sl). Open symbols represent measurements in the absence, whereas solid symbols represent data obtained in the presence (30 μM) of the drug. (A) The normalized inactivating component as a function of SR calcium release during the prepulse. Values obtained with a given membrane potential during the prepulse were averaged from eight fibers. For normalization the inactivating component of the nonconditioned (prepulse voltage = −100 mV) transient (P_0–Sl_0) was used. (B) Same data as in A, but calcium release during the prepulse was normalized to the maximal release in the given fiber as described in Fig. 5. (C) The suppression of the inactivating component, $\Delta(P–Sl) = (P_0–Sl_0) - (P–Sl)$, as a function of the inactivating component of the prepulse. Different symbols represent different fibers. Solid lines represent the least-squares fit of a linear function, constrained to go through the origin, to the data point with a slope of 0.973 and 1.088 in the presence and absence of thymol.

during the prepulse (Pizarro et al., 1997; Szentesi et al., 2000), in both cases.

These results clearly establish that the calcium-dependent inactivation of the calcium release channels is not suppressed in the presence of thymol. They, furthermore, argue in favor of the hypothesis that the drug does not influence the inactivation process of the channels at all, other than altering the $[Ca^{2+}]_i$ in the triadic junction.

Thymol induces a change in the transfer function

The data presented in the previous sections clearly demonstrate that thymol alters the way in which T-tubular depolarization affects the consequent increase in SR permeability. This alteration cannot be explained by the changes in the properties of intramembrane charge movement (see Fig. 1). To characterize the transmission of information from the T-tubular to the SR membrane, the transfer function of the triadic events, that is, SR permeability as a function of the amount of charge transferred, was calculated (Csernoch et al., 1999a).

Fig. 7 shows the change in transfer function induced by the application of 30 μM thymol. To obtain the data points, the mean normalized steady level of SR permeability was plotted as a function of the mean normalized charge. The presence of the drug clearly changed the coupling between charge movement and the SR permeability increase. As demonstrated in Fig. 1, the charge movement was practically unaffected by the thymol (slightly suppressed and shifted to the left), whereas the steady level of SR permeability was increased. This is evident from the transfer functions, which demonstrate that the same amount of charge moved brought about a larger calcium release in the presence of the drug. To describe the transfer function and the change induced by the thymol in detail, a straight line was fitted to the data points above the threshold for the appearance of detectable calcium release. The transfer function is then characterized by the slope (m) and the x-axis intercept ($Q_{th,r}$) of the straight line. The slope indicates the efficiency of the coupling whereas the intercept is the relative amount of charge moved before any measurable calcium release occurs. As the superimposed traces in Fig. 7 demonstrate, thymol increased the slope of the transfer function significantly, from 1.26 ± 0.09 to 2.37 ± 0.12, indicating a more efficient coupling between the voltage sensors and the calcium release channels. On the other hand, the drug did not alter $Q_{th,r}$ significantly (from 0.08 ± 0.06 to 0.16 ± 0.08).

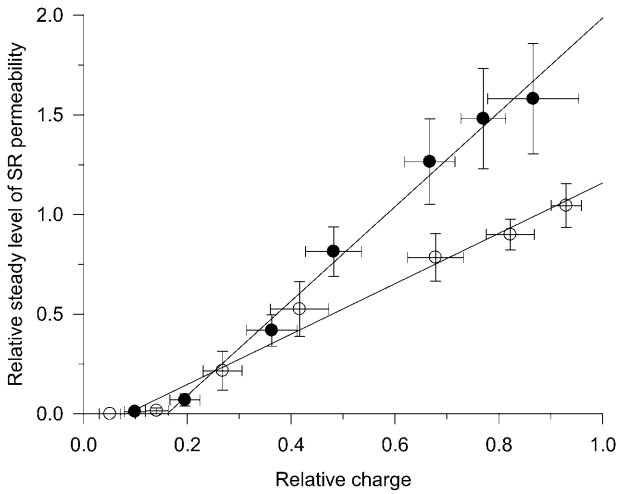

FIGURE 7 The change in transfer function induced by the application of 30 μM thymol. The mean steady level of SR permeability was plotted as a function of the mean normalized charge. The transfer function was characterized by the slope (m) and the x axis intercept ($Q_{th,r}$) of the straight line fitted to the data points. Thymol increased m (from 1.26 to 2.37), but did not significantly alter $Q_{th,r}$ (from 0.08 to 0.16) of the transfer function.

Thymol increases ryanodine binding to heavy SR vesicles

We have, so far, demonstrated that 30 μM thymol increases SR permeability by ~50% without altering the voltage-sensing function of the DHPRs. The results do not, however, exclude the presence of a putative binding site that might influence the interaction of DHPRs and RyRs. To exclude this possibility HSR vesicles were prepared and the effect of thymol was tested on ryanodine binding.

Ryanodine binding under control conditions was characterized by a single binding site (Fig. 8). The fit of Eq. 1 to data points in Fig. 8 *A* revealed a dissociation constant of 25.3 ± 1.4 nM and a B_{max} of 8.7 ± 0.3 pmol/mg protein. The presence of a single binding site per RyR was confirmed in the Scatchard plot (Fig. 8 *B*), where the straight line was constructed using the same parameters as above. The addition of 300 μM thymol caused a massive increase in ryanodine binding to HSR vesicles as demonstrated in Fig. 8, *A* and *B*. The drug increased both the affinity of the binding site (dissociation constant decreased to 15.5 ± 1.0 nM) and the amount bound (B_{max} increased to 14.7 ± 0.5 pmol/mg protein).

To describe the concentration dependence of thymol action, the amount of [^{3}H]ryanodine bound, at a concentration of 6 nM, was determined at different concentrations of thymol (Fig. 8 *C*). The data were then fitted with the Hill equation. This revealed a half-activating concentration of 144 ± 11 μM and a Hill coefficient of 1.89 ± 0.27.

Thymol was thus found to enhance ryanodine binding to HSR vesicles close to threefold. This observation, together with the results on SR permeability, points to a direct, stimulating action of thymol on the calcium release channel.

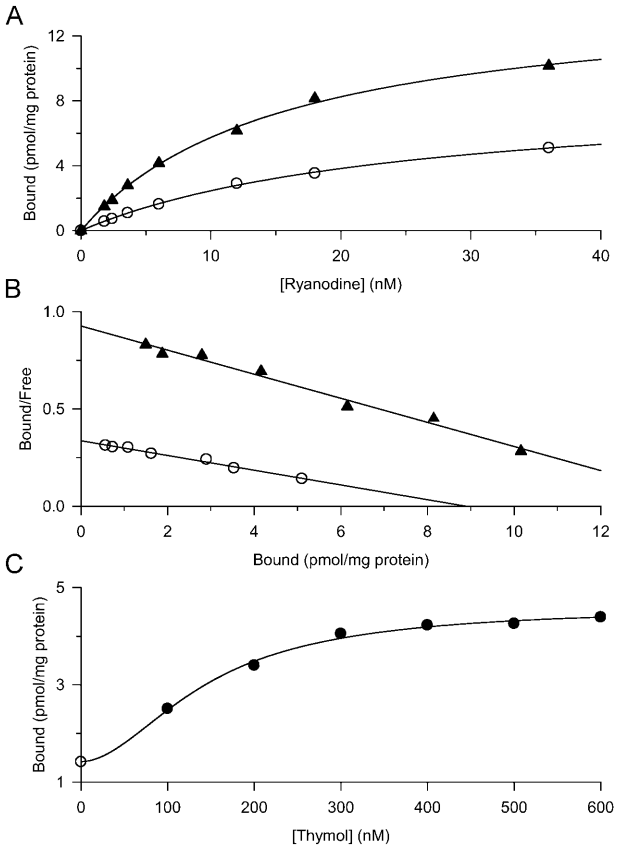

FIGURE 8 Effects of thymol on ryanodine binding to heavy SR vesicles. (*A*) Ryanodine binding determined in the absence (○) and presence (▲) of 300 μM thymol at different [^{3}H]ryanodine concentrations. Assuming a single binding site the Hill fit resulted in k_{50} = 25.3 ± 1.4 nM and B_{max} = 8.67 ± 0.26 pmol/mg protein in control, whereas k_{50} = 15.5 ± 1.0 nM and B_{max} = 14.65 ± 0.45 pmol/mg protein in the presence of the drug. (*B*) The data presented in *A* were used for constructing the Scatchard plot. Straight lines were drawn using the parameters given above. (*C*) Concentration-dependent effect of thymol on ryanodine binding. Ryanodine binding was determined in the absence and presence of various concentrations of thymol at 6 nM [^{3}H]ryanodine concentrations. Fitting the Hill equation resulted in a half-activating concentration of 144 ± 11 μM, a Hill coefficient of 1.89 ± 0.27, and approximately three times higher ryanodine binding at saturating thymol concentration than in control.

Thymol stimulates the isolated RyRs

To test the direct effect of thymol on the calcium release channel, isolated RyRs were incorporated into planar lipid bilayers and the properties of channel gating were determined. Under our experimental conditions the channels displayed a low open probability (P_o = 0.063 in Fig. 9 *A*). After the addition of 30 μM thymol the P_o increased (to 0.105 in Fig. 9 *B*), demonstrating a direct activating effect of the drug on the calcium release channel. This effect was present for all channels tested; the P_o increased from 0.089 ± 0.034 to 0.221 ± 0.044. Fig. 9 also demonstrates that thymol did not interfere with the ability of ryanodine to lock the calcium release channel in the characteristic, half-conducting state.

Examining the current records in Fig. 9, *A* and *B*, reveals that the size of the current, when the channel was open, was the same before and after the addition of the drug. This observation suggests that thymol does not influence the conductance of RyRs. This hypothesis was tested in the experiment presented in Fig. 9 *C*, where the current amplitude is plotted as a function of the holding potential both before (*open symbols*) and after (*solid symbols*) the addition of the drug. Fitting straight lines, constrained to go through the origin, to the data points, revealed a slope of 545 pS in control and 543 pS in the presence of the drug.

To further explore the action of thymol on channel gating the drug was applied in concentrations of 150 (Fig. 10 *B*) and 300 μM (Fig. 10 *C*). Together with the increased open probability long-lasting open events were observed. These events had, on average, the same lengths ($p > 0.4$) in the presence of 150 μM thymol (287 ± 21 s; 235 events) and in the presence of 300 μM thymol (317 ± 41 s; 159 events).

The experiments with isolated and reconstituted RyRs demonstrated that thymol is a potent activator of the calcium

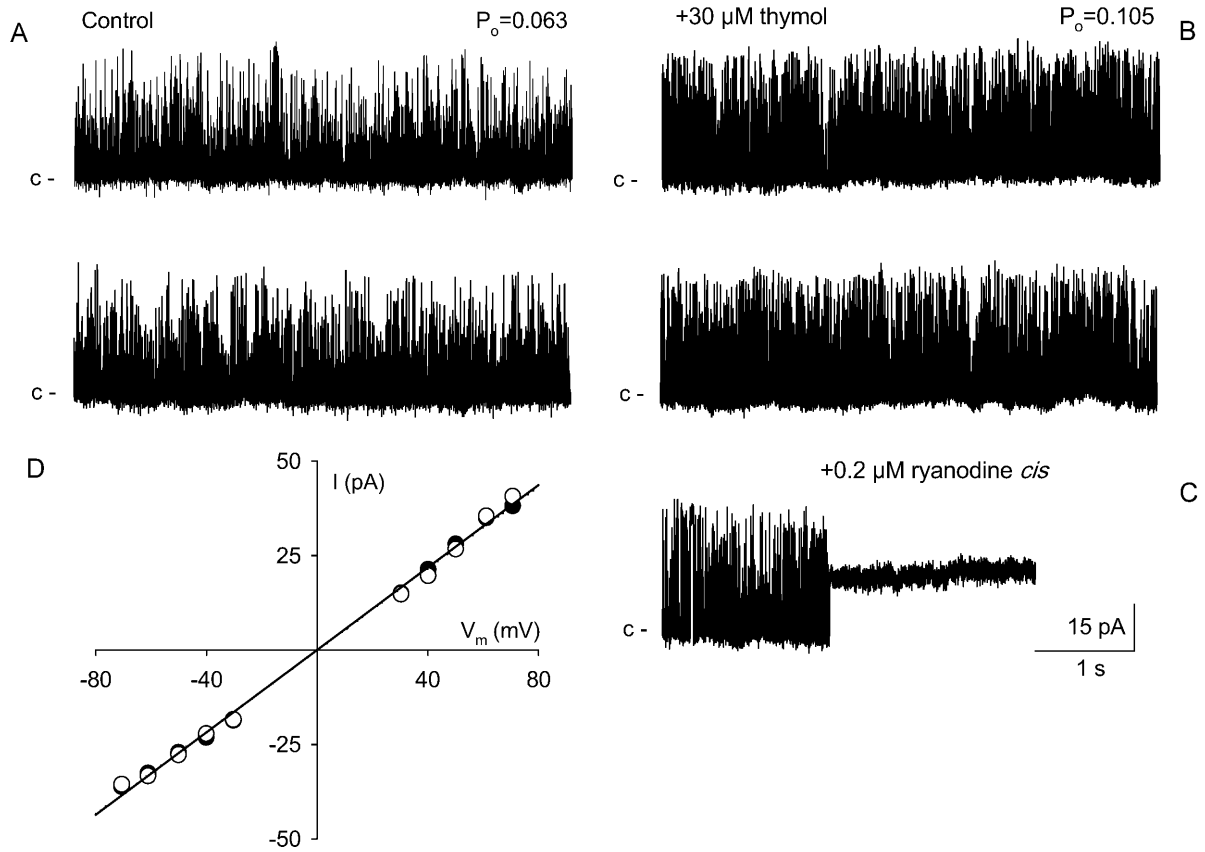

FIGURE 9 Effect of 30 μM thymol on the isolated RyRs. Incorporation was initiated in symmetric 250 mM KCl, holding potential was 61 mV; channel openings are upward deflections. Horizontal lines before each current record mark the closed state. (*A*) Single channel recordings in control conditions. (*B*) Representative segments of single channel behavior taken 5 min after the additions of thymol. (*C*) Single channel currents measured after the successive addition of 0.2 μM ryanodine into the *cis* chamber. (*D*) Single channel currents plotted as a function of the holding potential. Open symbols represent measurements under control conditions, whereas solid symbols represent those in the presence of thymol. Straight lines correspond to a single channel conductance of 545 and 543 pS in control and in the presence of the drug, respectively. All recordings are from a single experiment.

release channel—one which increases the open probability of the channel without significantly modifying the single channel conductance.

Elementary calcium release events are altered by thymol

Elementary calcium release events in mammalian muscle fibers exhibit a wide morphological variety. Calcium sparks, resembling those in frog fibers, can be preceded and/or followed by embers, or embers can occur on their own (Kirsch et al., 2001; Zhou et al., 2003). Since thymol was found to activate RyRs it was of interest to see if it modified the properties or appearance of the calcium release events. Calcium sparks and embers were thus measured on permeabilized fibers and their relative numbers and morphological properties compared in the absence and presence of the drug.

Under control conditions, calcium release events occurred with an appreciable frequency (0.0587 $\pm$ 0.0020 s^{-1} sarcomere^{-1}; Fig. 11 *A*) and displayed all the morphological characteristics described earlier (e.g., Kirsch et al., 2001). Most abundant were lone sparks (63%; Fig. 11 *Ba*), but lone embers (22%; Fig. 11 *Bb*) or sparks with trailing embers (Fig. 11 *Bc*) were also readily observable. Sparks with leading embers (Fig. 11 *Bd*) were rare (1.1% of all events). In the presence of thymol, the frequency increased to 0.0654 $\pm$ 0.0016 s^{-1} sarcomere^{-1} (Fig. 11 *C*; $p < 0.01$). More noticeable was the change in overall event characteristics, inasmuch as longer and more complex events dominated the images, with lone sparks (Fig. 11 *Da*) decreasing in relative proportion (41%). Lone embers (35%, Fig. 11 *Db*) and sparks with trailing embers (Fig. 11 *Dc*) were still readily distinguishable, with sparks with leading embers (Fig. 11 *Dd*) increasing in proportion to >4% of all events.

A total of 2030 vs. 2478 events from 20 vs. 9 fibers were analyzed under control conditions and in the presence of 30 μM thymol, respectively, and their characteristic parameters are presented in Table 3. The drug decreased the amplitude or average amplitude of both sparks and embers by 20–24% leaving the rise time and FWHM essentially constant. The decrease in spark amplitude was attributable to a decrease in

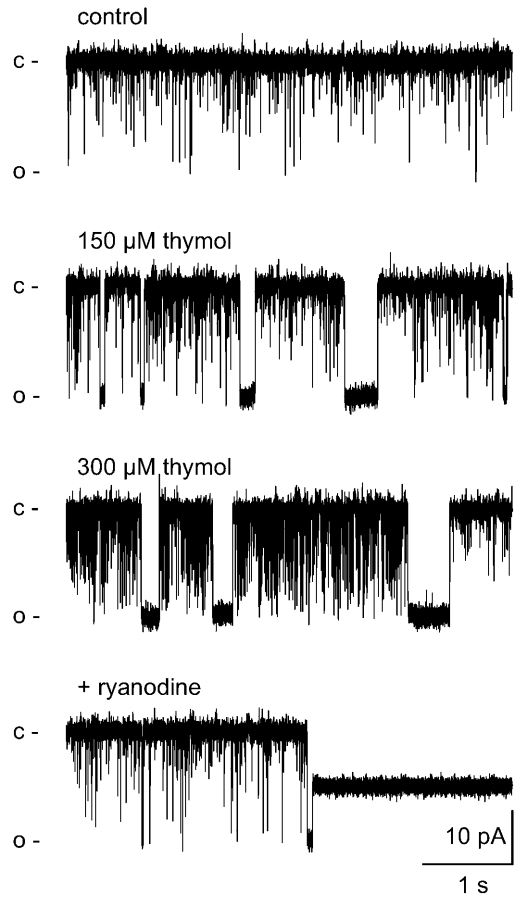

FIGURE 10 Effect of higher thymol concentrations on calcium release channel activity. Measurements were carried out under the same conditions as in Fig. 9 with the holding potential being −61 mV, and thus channel openings are downward deflections. Horizontal lines mark the closed state. The fast gating of the channel seen in control (*top*) is interrupted by long open events in the presence of both 150 (*second from top*) and 300 μM (*second from bottom*) thymol. Note that the channel opens to a full conducting state during the long open events. (*Bottom*) Ryanodine was capable of interfering with the thymol-induced alteration in channel gating. Note that the transition to the half-conducting state, characteristic to the ryanodine-modified channel, occurred during a long open event.

the number of large sparks as depicted in Fig. 11 *E*. In parallel, the duration of the calcium release events increased considerably. As evidenced from Fig. 12 and its inset, the drug, although reducing the relative proportion of shorter events, induced events that had durations of several hundred milliseconds.

Higher concentrations of thymol were found to induce long open events on isolated RyRs (Fig. 10). The application of 150 and especially 300 μM thymol to permeabilized fibers, to investigate their effects on elementary calcium release events, was in many cases disastrous. A massive release of calcium followed the addition of the drug, as evidenced from the sudden increase in fluorescence and contraction of the fiber (not shown). In only a few occasions were we successful in recording calcium release events in the presence of such high concentrations of the drug. Although this prevented a detailed statistical analysis, the events could still be characterized.

As shown in Fig. 12, sparks were hardly ever observed in the presence of 150 μM thymol. Rather, long events resembling lone embers were detected. Their duration, however, often exceeded 500 ms, sometimes lasting >1.5 s, the duration of the image. These events had characteristic amplitudes and full widths similar to the embers measured in the presence of low thymol concentrations. The fact that the amplitude of the fluorescence was steady over the entire event (Fig. 12) suggests that the channel(s) involved were continuously open.

These data clearly indicate that the long calcium release events correspond to the long-lasting open events seen for the thymol-modified isolated RyRs. Since the long calcium release events were neither preceded nor followed by a spark, they should be considered as the opening of a single release channel or the concerted opening of a small group of channels. It should be stressed, however, that were the latter the actual arrangement, the channels opening synchronously must always open together—which would constitute the elementary release unit. These findings thus strongly argue in favor of the lone ember being the elementary building block of calcium release in mammalian skeletal muscle.

DISCUSSION

These experiments give, for the first time, a complete account of the effects of thymol on steps of excitation-contraction coupling, from intramembrane charge movement to elementary calcium release events, in mammalian skeletal muscle fibers. Thymol was found to only slightly interfere with the voltage-sensing event but to augment SR calcium permeability by 50% already at 30 μM. The drug enhanced ryanodine binding to HSR vesicles by increasing both the affinity and the amount bound. The isolated and reconstituted calcium release channel displayed an increased open probability in the presence of thymol with the appearance of long-lasting open events at concentration above 100 μM. Elementary calcium release events were also modified in their characteristics with embers becoming more frequent and of longer duration. At high concentrations of thymol lone embers with extremely long duration dominated the images. These experiments argue that in mammalian skeletal muscle, embers arise from the opening of a single release channel, or a release unit, and thus represent the elementary event of calcium release.

Calcium release from the SR in the presence of thymol

Thymol has been known to affect calcium handling in a variety of cell types (Hisayama and Takayanagi, 1986; Kostyuk et al., 1991). In particular, Palade (1987) used it to

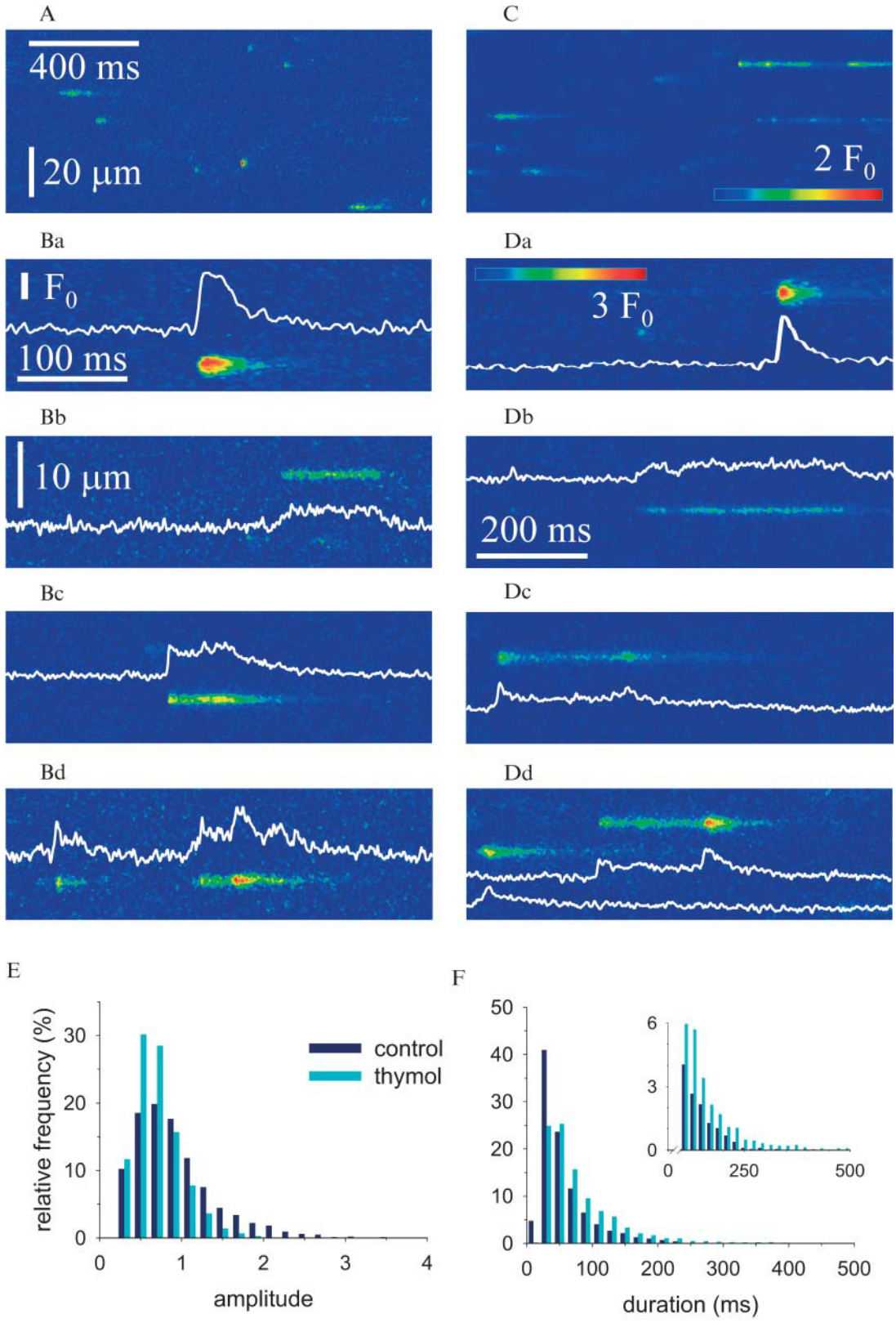

FIGURE 11 Modified elementary calcium release events in the presence of 30 μM thymol. (*A* and *B*) Calcium release events under control conditions. The large image (*A*) illustrates the frequency whereas the smaller images (*Ba–Bd*) demonstrate the wide variety in morphology of the events, namely, a lone spark (*Ba*), a lone ember (*Bb*), a spark with trailing (*Bc*), and a leading ember (*Bd*). (*C* and *D*) Calcium release events in the presence of thymol. The organization of the images is the same as in *A* and *B*, respectively. Note, however, the longer events in *Db–Dd*, characteristic to the thymol-treated cells. Traces in all images

TABLE 3 Thymol-induced changes in the morphological characteristics of elementary calcium release events

	Control		30 μM thymol	
	Spark ($n = 1576$)	Ember ($n = 454$)	Spark ($n = 1605$)	Ember ($n = 873$)
Amplitude	0.92 ± 0.01	0.210 ± 0.004	0.70 ± 0.01*	0.168 ± 0.002*
FWHM (μM)	1.81 ± 0.03	1.76 ± 0.03	1.74 ± 0.01*	1.77 ± 0.02
Rise time (ms)	9.4 ± 0.1	–	9.6 ± 0.1	–
Duration (ms)	56 ± 1	87 ± 2	79 ± 1*	102 ± 2*

Values represent mean ± SE. All events with sparks were grouped under Spark, whereas the parameters of lone embers are given under Ember. In the case of embers, the average amplitude is given.
*Significant differences between data in control and in the presence of thymol.

initiate calcium release from HSR vesicles isolated from rabbit skeletal muscle. Furthermore, thymol is used to stabilize liquid halothane, in which the added thymol can be as high as 0.1–0.7% (Thompson and Carlson, 1989). Taking the usual concentration of halothane in the in vitro contracture tests (1–2 mM), the thymol present can easily reach the concentration (30 μM) used in this study. Nevertheless, no account on the effects of the drug on SR calcium release has been published so far. Not only is this true for mammalian skeletal muscle, but to our knowledge, it is also true for striated muscle cells from other classes of vertebrates or invertebrates.

It is thus important to note that thymol, on its own, will facilitate calcium release from the SR, averaging an ~50% increase at 30 μM (see Table 2). In this respect its action is similar to that of caffeine (Klein et al., 1990; Csernoch et al., 1999a) or 4CmC (Struk and Melzer, 1999), although it seems to be more potent than either one. Its action further resembles that of caffeine inasmuch as 1), only slight differences between the effects of thymol on the two kinetic components, peak and steady level, of SR permeability (e.g., Table 2) were found and 2), the transfer function was altered in a way that suggests a more efficient coupling between the voltage sensors and the RyRs. These findings further strengthen the close and tight coupling between the two kinetic components of SR calcium release and favor the hypothesis that they both originate from the skeletal isoform of RyRs. Nevertheless, the mode of action of thymol is clearly distinct from that of caffeine or 4CmC, as evidenced from its effects on RyRs.

Effects of thymol on RyRs

Thymol is known to induce calcium release from heavy SR vesicles and was thus used in previous experiments to assess the action of other drugs on RyR function (Palade, 1987; Szentesi et al., 2001). Those experiments used concentrations of 300 μM. Data from [^{3}H]ryanodine binding experiments presented in this study (Fig. 8) demonstrate that thymol in that concentration would cause an approximately threefold increase in ryanodine binding, which is close to its maximal effect.

The half-activating concentration of thymol in the [^{3}H]ryanodine binding experiments was found to be 144 μM. This is approximately fivefold higher than the concentration in which the drug was capable of augmenting the calcium transients (Fig. 2) or SR calcium release (Fig. 3). On the other hand, it is consistent with the observation that the resting $[Ca^{2+}]_i$ was only slightly (20 nM) elevated by the drug in this low concentration. One would predict, based on these data, that higher concentrations of thymol, especially at several hundred μM, will initiate large efflux of calcium from the SR even under resting conditions and would, therefore, hinder the comparison of SR calcium release in control conditions and in the presence of the drug. Due to this foreseen difficulty such experiments were not included in the present study.

The [^{3}H]ryanodine binding data, however, call attention to an additional point. The Hill coefficient of thymol action was found to be 1.89—that is, close to 2 (see Fig. 8). This indicates that two thymol molecules, acting cooperatively, are needed to induce the observed stimulating effect.

Analyzing the action of 30 μM thymol on the isolated and reconstituted RyRs revealed an ~60% increase in open probability (Fig. 9) with no change in single channel conductance. In this respect the effect of the drug is similar to that of caffeine (Rousseau et al., 1988) or 4CmC (Herrmann-Frank et al., 1996). Unlike 4CmC or caffeine, however, thymol was found to induce long-lasting open events, which raises the need for finding an alternative explanation for its mode of action. Such alternative explanation could be based on the antioxidant effect of the drug since the calcium release channel is regulated by its redox state (e.g., Feng et al., 2000; Sun et al., 2001). Although possible redox regulation of SR calcium release will be discussed later it should be mentioned here that sulfhydryl

(*A–D*) represent the timecourse of F/F_0 measured at the position of the peak (events with spark) or in the middle of the event (lone ember) by averaging three neighboring pixels in the *x* direction. (*E*) Relative distribution of the amplitudes of events with sparks. (*F*) Relative distribution of the duration of all events. Inset shows the lower portion of the graph to demonstrate the presence of events with long duration in the presence of the drug.

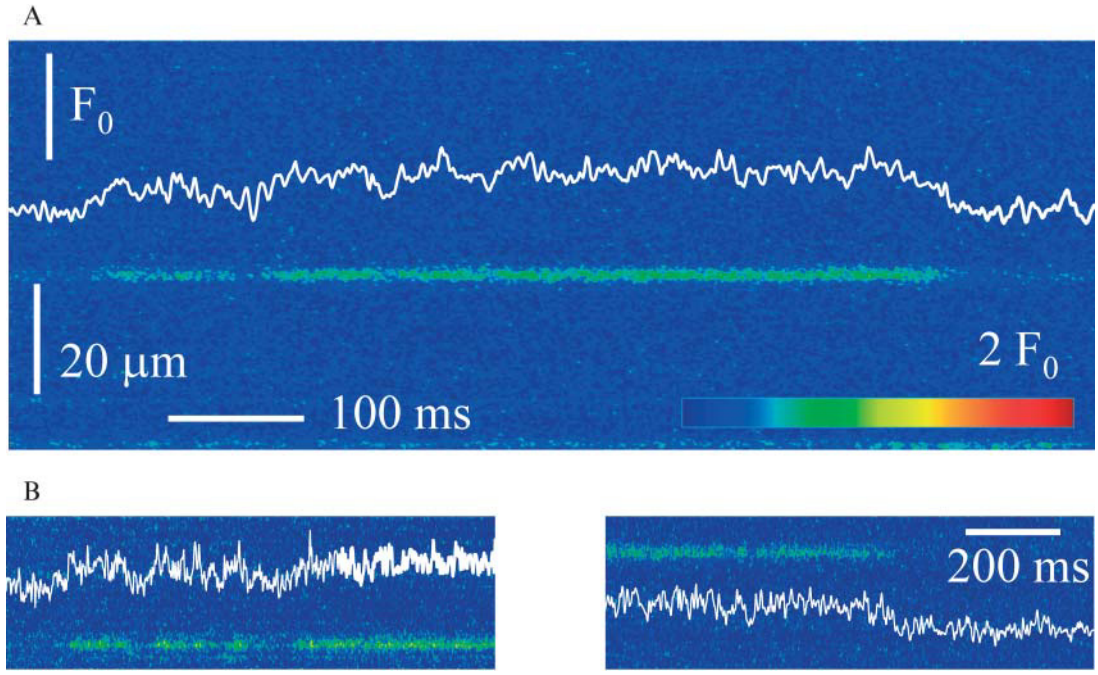

FIGURE 12 Calcium release events in the presence of 150 μM thymol. Representative images showing events with extremely long duration, otherwise resembling embers measured under control conditions. Note that the fluorescence (F/F_0) and the spatial width of these long events stay essentially constant over hundreds of milliseconds (*A*). Note also that the release unit can reopen (*B*) and give rise to an event with the same spatial and temporal characteristics. Traces in the images were calculated as described in Fig. 11 for lone embers.

oxidation, rather than reduction, was found to increase the P_o of the reconstituted channel (e.g., Suko et al., 2000).

On the other hand, the long-lasting open events with full conductance observed in the presence of thymol resemble those measured with bastadin 10 (Chen et al., 1999). The effects of bastadin 10 were interpreted as a shift in the free energy of the open state of the drug-modified RyRs. Furthermore, the removal of FKBP12 from the RyRs interfered with the action of bastadin 10 (Chen et al., 1999). Although the present experiments did not test the FKBP12 sensitivity of effect of thymol, it is, nevertheless, likely that the two drugs share the capability of lowering the free energy of the open state of RyRs.

As mentioned above, the value of close to 2 for the Hill coefficient indicates that two thymol-binding sites are present for each calcium release channel. Noteworthy is the observation that channel activity in between long-lasting open events, in the presence of higher thymol concentrations, was found to have higher open probability than in control conditions. This raises the possibility that the binding of the first thymol molecule would already activate the channel and thus increase its P_o. The binding of the second molecule could then shift the channel to the long-lasting open state.

Effects of thymol on DHPR function

To our knowledge no previous work has examined the effects of thymol on the voltage sensor of E-C coupling. Recent experiments have, on the other hand, demonstrated that the L-type calcium currents from cardiac (Magyar et al., 2002) as well as skeletal (Szentandrássy et al., 2003) muscle are suppressed by the drug. Thymol neither altered the voltage dependence of current activation nor the reversal potential for calcium, but attenuated the conductance of the channels. In cardiac preparations the voltage dependence of steady-state inactivation was shifted to more negative membrane potentials (Magyar et al., 2002). In the above changes thymol had a half-effective concentration ~200 μM. In the experiments presented here thymol failed to induce marked alterations in intramembrane charge movement even at 300 μM (Fig. 1 and Table 1). Since Q_{max} did not change significantly it cannot account for the >50% reduction in conductance seen in the previous reports. This observation suggests that either the alteration described for the calcium current represents specific effects of thymol on ion permeation of the L-type calcium channels or, alternatively, that intramembrane charge movement and L-type calcium current originate from distinct subpopulations of DHPRs.

To interpret the slight change in the voltage dependence of intramembrane charge movement (see Fig. 1 *B* and Table 1) one should consider the large amount of evidence supporting the idea that altered SR calcium release influences intramembrane charge movement (Pizarro et al., 1991; Pape et al., 1996; Shirokova and Ríos, 1996). Results obtained here, such as little effect on Q_{max} and a

leftward shift in V_{50}, closely resemble those published earlier for compounds such as caffeine or perchlorate that enhance SR calcium release (e.g., González and Ríos, 1993; Csernoch et al., 1999a). Noteworthy here is the observation that intramembrane charge movement displayed clear delayed components in the presence of thymol (see Fig. 1). This again is consistent with previous data suggesting that calcium released from the SR influences charge movement (e.g., Pizarro et al., 1991). It should be stressed, however, that mammalian fibers under control conditions hardly ever show such slow components on their charge movement currents (e.g., Szentesi et al., 1997). The observation that thymol can alter charge movement in such a way that this component becomes visible suggests that it is present in mammalian muscle, albeit masked under control conditions.

Redox regulation of the calcium release channel

Thymol, under most conditions, is used as an antioxidant. A number of studies have called the attention to the redox sensor function of RyRs (e.g., Abramson and Salama, 1988; Marengo et al., 1998). The calcium release channel is known to contain a large number of reactive cysteines, a number of which can undergo oxidation or reduction under appropriate conditions (Moore et al., 1999; Sun et al., 2001). RyRs were, recently, shown to respond to changes in the redox state of the intracellular environment and thus serve as a redox sensor (Feng et al., 2000; Xia et al., 2000). Changes in the redox potential established across the SR membrane by the reduced and oxidized forms of glutathione, as well as the oxidation or reduction of reactive cysteines on the RyRs, have also been shown to alter the open probability of the calcium release channel (Feng et al., 2000; Sun et al., 2001). The fact that most studies on SR calcium release in intact or cut fiber preparations were conducted under ambient oxygen levels, whereas in situ functioning muscle is an environment with much lower oxygen content and antioxidants such as methyl *p*-hydroxybenzoate (Cavagna et al., 2000) and thymol (this study) alter RyR function and SR calcium release, makes the question of redox regulation even more intriguing.

On the other hand, the treatment of mechanically skinned mammalian fibers working at ambient oxygen levels with the strong oxidant H_2O_2 increased, rather than reduced, SR calcium release (Posterino et al., 2003). Furthermore, reducing reagents (as dithiothreitol or reduced glutathione) affected the calcium sensitivity of the contractile apparatus and not the calcium release process (Posterino et al., 2003). Finally, the massive release of calcium from the SR in the presence of larger thymol concentrations cannot be explained in a framework where the drug would solely relieve a block caused by massive oxidation. Taken the above, alternative explanations must be considered to understand the effects of thymol.

Due to its lipid solubility thymol is expected to enter all membranes and possibly influence their fluidity and thus the interaction between the membrane and its integral proteins, channels, and pumps. Work on aging rats has indeed revealed that the administration of thyme oil (or thymol itself) can have beneficial effect on the polyunsaturated fatty acid composition of certain membranes (Youdim and Deans, 1999). This raises the possibility that the actions of thymol seen at larger ($>100\ \mu$M) concentrations are influenced by thymol's effect on the lipids or on the lipid-protein interaction resulting, as discussed above, in the reduction of the free energy associated with the open state of the channel.

Calcium release events in permeabilized fibers

Elementary calcium release events in mammalian skeletal muscle preparations have recently been reported from a number of laboratories (Conklin et al., 2000; Kirsch et al., 2001; Zhou et al., 2003). These events differ from those measured in amphibians (Tsugorka et al., 1995, Klein et al, 1996) mainly in their morphological variability, namely, that sparks and embers coexist, and in their relative frequency, events are more numerous in frogs. In line with previous studies (e.g., Shirokova et al., 1998) we were also unable to detect calcium sparks in intact (Fluo-3 AM loaded) or notched fibers (data not shown) and, therefore, followed the idea of Kirsch et al. (2001) to chemically skin the fibers. The removal of the surface membrane with saponin proved to be successful, and elementary calcium release events were recorded routinely on these fibers. However, their frequency was still far too low to enable decent statistical comparison between control and drug-modified states. To increase the number of events the measurements were carried out with sulfate as the major anion in the bathing solution. This indeed resulted in an appreciable frequency (Fig. 11) without any marked alterations in the characteristics of the events as described earlier (Csernoch et al., 2003).

Under these conditions the proportion of events with embers (lone embers and sparks with embers) was found to be 37% (22% for lone embers) in good agreement with the report by Zhou and collaborators (2003), but slightly lower than that reported by Kirsch et al. (2001; 33% for lone embers). It should be noted, however, that the composition of the solutions used here more closely resembled that applied in the former study and, furthermore, a similar automatic computerized detection method was used.

The calcium sparks and embers detected in this study were morphologically similar to those reported earlier. They had a smaller average amplitude than those reported by Kirsch et al. (2001), as expected from the use of sulfate and the consequent lowering of the SR calcium content due to the precipitation of $CaSO_4$ inside the SR (Csernoch et al., 2003). The measured FWHM and rise time were essentially identical with previous values, although the FWHM more

closely resembled the value reported by Kirsch et al. (2001; 1.85 μm) than that reported by Csernoch et al. (2003; 2.04 μm). Noteworthy is the difference that Kirsch et al. (2001) found it sufficient to draw an *FDHM* (full duration at half-maximum) $>$ 50 ms selection criteria for distinguishing embers from sparks, whereas here, lone embers shorter than 50 ms were, occasionally, also observed. Taken together, the methods used here were clearly capable of detecting elementary calcium release events with the spatial and temporal characteristics observed on previous occasions. This enabled us to compare the events before and after the addition of thymol and to analyze the action of the drug.

Calcium release events in the presence of thymol

Thymol, in a concentration of 30 μM, has slightly increased the frequency of the elementary calcium release events, from 0.0587 to 0.0654 s^{-1} sarcomere^{-1}, which is in agreement with its effects on the calcium release measured on cut fibers and on the open probability of isolated RyRs. The increase in event frequency was, however, not as marked as the increase in global calcium release. Nevertheless, the relative proportion of embers, which, as it will be discussed later, are more likely to be the elementary events in mammals, were increased more than the actual frequency.

In higher concentrations the drug resulted, in most cases, in a massive release of calcium, rendering the detection of individual events impossible. (This global release could be interpreted as a drastic increase in event frequency, in line with the effects described above.) In the few cases where the fiber survived the addition of 150 μM thymol, the frequency of the events was reduced and the relative proportion of embers was further increased.

Comparing the average amplitudes of sparks or embers before (0.93 and 0.21) and after (0.70 and 0.17) the addition of thymol (Table 3) reveals a 20–24% decrease in both cases. This suppression of event amplitude can only be explained as a drop in SR content due to an increased leak of calcium from the SR. Together with the decrease in amplitude, the rise time and the duration of events were increased from 9.4 to 9.6, and from 56 to 79 ms, respectively. The increase in rise time and duration is, on the one hand, likely to be due to the effect of thymol on the open time of the release channel. On the other hand, the decrease in the amplitude of sparks reflects a lower concentration of calcium at the release site and, therefore, a possibly less prominent negative feedback of the released calcium.

The number of channels involved in the generation of a spark in mammalian muscle

One of the most intriguing findings of this study is the appearance of long events observed in the presence of thymol, especially with the higher, 150 μM, concentration of the drug. These calcium release events resemble those measured in frog skeletal muscle treated with imperatoxin A (González et al., 2000a; Shtifman et al., 2000) or bastadin 10 (González et al., 2000a). They are most likely due to the drug-induced alteration in channel gating, namely, the long-lasting open events seen in lipid bilayer experiments. The fact that the calcium release events displayed steady fluorescence and essentially equal spatial width during their entire timecourse implies that the released calcium reached a steady state with the diffusion and binding of calcium.

Unlike imperatoxin, which locks the channel in a subconductance state (Tripathy et al., 1998), but similarly to bastadin 10 (Chen et al., 1999), thymol did not affect the conductance of the channel. The change in fluorescence during the long events should, therefore, provide an upper limit to the ΔF, if a single channel, or the elementary release unit if it is more than a single channel, opens to a full conductance state. Since the embers measured in the absence of the drug had an average amplitude comparable to that of the long events—the slight difference, as discussed above, is most likely due to the difference in SR contents—they must represent the opening of an elementary release unit under control conditions. This unit must either 1), consist of a single channel, inasmuch as no stepwise increase (only occasional closings as in Fig. 12 *B*) in fluorescence was observed during the long events that could have indicated the opening or closing of a channel or 2), the channels involved gate synchronously (Marx et al., 1998; Zhou et al., 2003).

To estimate the number of channels involved in generating a spark, note that the largest sparks had an average amplitude of 2.96 and a FWHM of 2.09 μm (15 largest events). Similar parameters for large embers were 0.43 and 1.72 μm, respectively. As discussed earlier (e.g., Ríos et al., 1999; Jiang et al., 1999) large events represent scans close to the source and, therefore, give the best possible resolution. Signal mass (*SM*; introduced by Sun et al., 1998) was shown to be proportional to the amplitude and FWHM^3 (Chandler et al., 2003), whereas its first derivative is at the onset of the event to release current (ZhuGe et al., 2000). It follows, therefore, that the ratio of release currents, and thus of the number of channels (N) involved, is

$$N_s/N_e = \{d(A_s \times FWHM_s^3)/dt\}/\{d(A_e \times FWHM_e^3)/dt\}, \quad (4)$$

where the subscripts s and e denote spark and ember, respectively, and A and *FWHM* should be calculated for every time point.

There are two possible routes to evaluate Eq. 4. In the direct approach, A and *FWHM* are determined by fitting Gaussian functions to each line, $F[x,t = constant]$, in the line-scan image. SM is then plotted as a function of time and its derivative is calculated. For the above-mentioned sparks and embers, the rate of change in SM was found to be on average 8.4 $\pm$ 1.0 and 0.29 $\pm$ 0.7 pl s^{-1}, respectively. This

yields 29 for the relative number of channels involved in generating a spark. Note, however, that the scatter for $d(SM)/dt$ for embers is large. This is due to the poor estimation of the parameters of the Gaussian function since, for these small events, the signal/noise ratio is high.

The indirect approach utilizes the observation that SM increases linearly in time until the channel is open, inasmuch as channel conductance remains the same and no appreciable depletion occurs at early times. Therefore SM measured at the time of the peak and divided by the rise time is a good estimate of $d(SM)/dt$. Note also that the time to reach steady width for the large embers (10 ms) was comparable with the rise time of the large sparks (9 ms). Since the spatial spread of embers reaches a maximum and then stays constant thereafter, FWHM, calculated as described in Methods, represents the upper limit of FWHM during the evolution of the ember. Thus the indirect approach gives a simple way to get a lower limit for N_s over N_e. With the data given above for A and $FWHM$, N_s over N_e calculates to be 11 in agreement with the value obtained with the direct method.

In other words, ~20–30 times more channels open during a spark than during an ember. If embers represent single channel events, sparks are generated when some 20–30 channels open. On the other hand, if embers are generated by a number of synchronously opening channels, the number of channels opened during a spark could easily reach 100—that is, the entire couplon (Stern et al., 1997).

On the other hand, following the line of reasoning given by ZhuGe et al. (2000), one can estimate $d(SM)/dt$ for a single channel. Using 0.5 pA for single channel current, 150 nM free $[Ca^{2+}]_i$ and 100 μM for the concentration of the dye $d(SM)/dt$ calculates to be 0.18 pl s^{-1}. This value suggests that 1–2 channels are involved in generating an ember and some 50 channels in generating a spark.

These experiments have demonstrated that thymol enhances SR calcium release by acting directly on the RyR calcium release channels. On purified channels reconstituted into lipid bilayers it increases the open probability and induces long-lasting open events. In parallel, elementary calcium release events with long duration, resembling embers, are observed in line-scan images. These data constitute the first full description, from the voltage-sensing event to calcium release, of drug-modified E-C coupling in mammalian skeletal muscle and give an experimental estimation of the relative number of release channels involved in generating a mammalian spark. They also argue in favor of the ember representing the opening of the elementary calcium release unit, either as a single channel or a group of channels always opening together, in mammalian skeletal muscle.

The authors thank Ms. R. Őri and É. Sági for skillful technical assistance.

This work was supported by research grants from the Hungarian government (OTKA T034894, T037727, and TS040773; FKFP 0193/2001; and ETT 250/2003).

REFERENCES

Abramson, J. J., and G. Salama. 1988. Sulfhydryl oxidation and Ca^{2+} release from sarcoplasmic reticulum. *Mol. Cell Biochem.* 82:81–84.

Cavagna, D., F. Zorzato, E. Babini, G. Prestipino, and S. Treves. 2000. Methyl *p*-hydroxybenzoate (E-218) a preservative for drugs and food is an activator of the ryanodine receptor Ca^{2+} release channel. *Br. J. Pharmacol.* 131:335–341.

Chandler, W. K., S. Hollingworth, and S. M. Baylor. 2003. Simulation of calcium sparks in cut skeletal muscle fibers of the frog. *J. Gen. Physiol.* 121:311–324.

Chen, L., T. F. Molinski, and I. N. Pessah. 1999. Bastadin 10 stabilizes the open conformation of the ryanodine-sensitive Ca^{2+} channel in an FKBP12-dependent manner. *J. Biol. Chem.* 274:32603–32612.

Cheng, H., W. J. Lederer, and M. B. Cannel. 1993. Calcium sparks: elementary events underlying excitation-contraction coupling in heart muscle. *Science.* 262:740–744.

Cheng, H., L. S. Song, N. Shirokova, A. González, E. G. Lakatta, E. Ríos, and M. D. Stern. 1999. Amplitude distribution of calcium sparks in confocal images. Theory and studies with an automatic detection method. *Biophys. J.* 76:606–617.

Conklin, M. W., C. A. Ahern, P. Vallejo, V. Sorrentino, H. Takeshima, and R. Coronado. 2000. Comparison of Ca^{2+} sparks produced independently by two ryanodine receptor isoforms (type 1 or type 3). *Biophys. J.* 78:1777–1785.

Csernoch, L., P. Szentesi, and L. Kovács. 1999a. Differential effects of caffeine and perchlorate on excitation-contraction coupling in mammalian skeletal muscle. *J. Physiol.* 520:217–230.

Csernoch, L., P. Szentesi, S. Sárközi, C. Szegedi, and I. Jona. 1999b. Effects of tetracaine on sarcoplasmic calcium release in mammalian skeletal muscle fibers. *J. Physiol.* 515:843–857.

Csernoch, L., P. Szentesi, and L. Kovács. 2002. Increased calcium release from the sarcoplasmic reticulum (SR) in the presence of thymol in mammalian skeletal muscle fibers. *Biophys. J.* 21:641a.

Csernoch, L., J. Zhou, B. Launikonis, A. González, M. D. Stern, G. Brum, and E. Ríos. 2003. The effects of SO_4^{2-}, a Ca^{2+}-precipitating buffer, on Ca^{2+} sparks of mammalian and batrachian twitch muscle. *Biophys. J.* 84:386a.

Feng, W., G. Liu, P. D. Allen, and I. N. Pessah. 2000. Transmembrane redox sensor of ryanodine receptor complex. *J. Biol. Chem.* 275:35902–35907.

Fusi, F., S. Saponara, H. Gagov, and G. Sgaragli. 2001. Effects of some sterically hindered phenols on whole-cell Ca^{2+} current of guinea-pig gastric fundus smooth muscle cells. *Br. J. Pharmacol.* 132:1326–1332.

González, A., W. G. Kirsch, N. Shirokova, G. Pizarro, G. Brum, I. N. Pessah, M. D. Stern, H. Cheng, and E. Ríos. 2000a. Involvement of multiple intracellular release channels in calcium sparks of skeletal muscle. *Proc. Natl. Acad. Sci. USA.* 97:4380–4385.

González, A., W. G. Kirsch, N. Shirokova, G. Pizarro, M. D. Stern, and E. Ríos. 2000b. The spark and its ember: separately gated local components of Ca^{2+} release in skeletal muscle. *J. Gen. Physiol.* 115:139–158.

González, A., and E. Ríos. 1993. Perchlorate enhances transmission in skeletal muscle excitation-contraction coupling. *J. Gen. Physiol.* 102: 373–421.

Herrmann-Frank, A., M. Richter, S. Sárközi, U. Mohr, and F. Lehmann-Horn. 1996. 4-Chloro-*m*-cresol, a potent and specific activator of the skeletal muscle ryanodine receptor. *Biochim. Biophys. Acta.* 1289:31–40.

Hisayama, T., and I. Takayanagi. 1986. Some properties and mechanisms of thymol-induced release of calcium from the calcium-store in guinea-pig taenia caecum. *Jpn. J. Pharmacol.* 40:69–82.

Jiang, Y.-H., M. G. Klein, and M. F. Schneider. 1999. Numerical simulation of Ca^{2+} ''sparks'' in skeletal muscle. *Biophys. J.* 77:2333–2357.

Kirsch, W. G., D. Uttenweiler, and R. H. A. Fink. 2001. Spark- and ember-like elementary Ca^{2+} release events in skinned fibres of adult mammalian skeletal muscle. *J. Physiol.* 537:379–389.

Klein, M. G., H. Cheng, L. F. Santana, Y.-H. Jiang, W. J. Lederer, and M. F. Schneider. 1996. Two mechanisms of quantized calcium release in skeletal muscle. *Nature*. 379:455–458.

Klein, M. G., B. J. Simon, and M. F. Schneider. 1990. Effects of caffeine on calcium release from the sarcoplasmic reticulum in frog skeletal muscle fibers. *J. Physiol*. 425:599–626.

Koshita, M., and T. Oba. 1989. Caffeine treatment inhibits drug-induced calcium release from sarcoplasmic reticulum and caffeine contracture but not tetanus in frog skeletal muscle. *Can. J. Physiol. Pharmacol*. 67:890–895.

Kostyuk, P. G., P. V. Belan, and A. V. Tepikin. 1991. Free calcium transients and oscillations in nerve cells. *Exp. Brain Res*. 83:459–464.

Magyar, J., N. Szentandrássy, T. Bányász, L. Fülöp, A. Varró, and P. P. Nánási. 2002. Effects of thymol on calcium and potassium currents in canine and human ventricular cardiomyocytes. *Br. J. Pharmacol*. 136:330–338.

Marengo, J. J., C. Hidalgo, and R. Bull. 1998. Sulfhydryl oxidation modifies the calcium dependence of ryanodine-sensitive calcium channels of excitable cells. *Biophys. J*. 74:1263–1277.

Marx, S. O., K. Ondrias, and A. R. Marks. 1998. Coupled gating between individual skeletal muscle Ca^{2+} release channels (ryanodine receptors). *Science*. 281:818–821.

Meissner, G. 1994. Ryanodine receptor/Ca^{2+} release channels and their regulation by endogenous effectors. *Annu. Rev. Physiol*. 56:485–508.

Moore, C. P., J.-Z. Zhang, and S. L. Hamilton. 1999. A role for cysteine 3635 of RYR1 in redox modulation and calmodulin binding. *J. Biol. Chem*. 274:36831–36834.

Palade, P. 1987. Drug-induced Ca^{2+} release from isolated sarcoplasmic reticulum. II. Releases involving a Ca^{2+} induced Ca^{2+} release channel. *J. Biol. Chem*. 262:6142–6148.

Pape, P. C., D. S. Jong, and W. K. Chandler. 1996. A slow component of intramembranous charge movement during sarcoplasmic reticulum calcium release in frog cut muscle fibers. *J. Gen. Physiol*. 107:79–101.

Pizarro, G., L. Csernoch, I. Uribe, M. Rodriguez, and E. Ríos. 1991. The relationship between Q_γ and Ca release from the sarcoplasmic reticulum in skeletal muscle. *J. Gen. Physiol*. 97:913–947.

Pizarro, G., N. Shirokova, A. Tsugorka, and E. Ríos. 1997. ''Quantal'' calcium release operated by membrane voltage in frog skeletal muscle. *J. Physiol*. 501:289–303.

Posterino, G. S., M. A. Cellini, and G. D. Lamb. 2003. Effects of oxidation and cytosolic redox conditions on excitation-contraction coupling in rat skeletal muscle. *J. Physiol*. 547:807–823.

Ríos, E., and G. Pizarro. 1991. Voltage sensor of excitation-contraction coupling in skeletal muscle. *Physiol. Rev*. 71:849–908.

Ríos, E., M. D. Stern, A. Gonzáles, G. Pizarro, and N. Shirokova. 1999. Calcium release flux underlying Ca^{2+} sparks of frog skeletal muscle. *J. Gen. Physiol*. 114:31–48.

Rousseau, E., J. LaDine, Q. Y. Liu, and G. Meissner. 1988. Activation of the Ca^{2+} release channel of skeletal muscle sarcoplasmic reticulum by caffeine and related compounds. *Arch. Biochem. Biophys*. 267:75–86.

Shirokova, N., J. García, and E. Ríos. 1998. Local calcium release in mammalian skeletal muscle. *J. Physiol*. 512:377–384.

Shirokova, N., and E. Ríos. 1996. Caffeine enhances intramembranous charge movement in frog skeletal muscle by increasing cytoplasmic Ca^{2+} concentration. *J. Physiol*. 493:341–356.

Shtifman, A., C. W. Ward, J. Wang, H. H. Valdivia, and M. F. Schneider. 2000. Effects of imperatoxin A on local sarcoplasmic reticulum Ca^{2+} release in frog skeletal muscle. *Biophys. J*. 79:814–827.

Simon, B. J., M. G. Klein, and M. F. Schneider. 1991. Calcium dependence of inactivation of calcium release from the sarcoplasmic reticulum in skeletal muscle fibers. *J. Gen. Physiol*. 97:437–471.

Stern, M. D., G. Pizarro, and E. Ríos. 1997. Local control model of excitation-contraction coupling in skeletal muscle. *J. Gen. Physiol*. 110: 415–440.

Struk, A., and W. Melzer. 1999. Modification of excitation-contraction coupling by 4-chloro-*m*-cresol in voltage-clamped cut muscle fibers of the frog (*R. pipiens*). *J. Physiol*. 515:221–231.

Suko, J., G. Hellmann, and H. Drobny. 2000. Modulation of the calmodulin-induced inhibition of sarcoplasmic reticulum calcium release channel (ryanodine receptor) by sulfhydryl oxidation in single channel current recordings and [^{3}H]ryanodine binding. *J. Membr. Biol*. 174:105–120.

Sun, J., L. Xu, J. P. Eu, J. S. Stamler, and G. Meissner. 2001. Classes of thiols that influence the activity of the skeletal muscle calcium release channel. *J. Biol. Chem*. 276:15625–15630.

Szegedi, C., S. Sárközi, A. Herzog, I. Jona, and M. Varsanyi. 1999. Calsequestrin: more than ''only'' a luminal Ca^{2+} buffer inside the sarcoplasmic reticulum. *Biochem. J*. 337:19–22.

Szentandrássy, N., P. Szentesi, J. Magyar, P. P. Nanasi, and L. Csernoch. 2003. Effect of thymol on kinetic properties of Ca and K currents in rat skeletal muscle. *BMC Pharmacology*. 3:9.

Szentesi, P., C. Collet, S. Sárközi, C. Szegedi, I. Jona, V. Jacquemond, L Kovács, and L. Csernoch. 2001. Effects of dantrolene on steps of excitation-contraction coupling in mammalian skeletal muscle fibers. *J. Gen. Physiol*. 118:355–375.

Szentesi, P., V. Jacquemond, L. Kovács, and L. Csernoch. 1997. Intramembrane charge movement and sarcoplasmic calcium release in enzymatically isolated mammalian skeletal muscle fibers. *J. Physiol*. 505:371–384.

Szentesi, P., L. Kovács, and L. Csernoch. 2000. Deterministic inactivation of calcium release in mammalian skeletal muscle. *J. Physiol*. 528:447–456.

Sun, X.-P., N. Callamaras, J. S. Marchant, and I. Parker. 1998. A continuum of $InsP_3$-mediated elementary Ca^{2+} signalling events in *Xenopus* oocytes. *J. Physiol*. 509:67–80.

Thompson, R. D., and M. Carlson. 1989. Determination of thymol in halothane anaesthetic preparations by high-performance liquid chromatography. *J. Pharm. Biomed. Anal*. 7:1199–1206.

Tripathy, A., and G. Meissner. 1996. Sarcoplasmic reticulum luminal Ca^{2+} has access to cytosolic activation and inactivation sites of skeletal muscle Ca^{2+} release channel. *Biophys. J*. 70:2600–2615.

Tripathy, A., W. Resch, L. Xu, H. H. Valdivia, and G. Meissner. 1998. Imperatoxin A induces subconductance states in Ca^{2+} release channels (ryanodine receptors) of cardiac and skeletal muscle. *J. Gen. Physiol*. 111:679–690.

Tsugorka, A., E. Ríos, and L. A. Blatter. 1995. Imaging elementary of calcium release in skeletal muscle cells. *Science*. 269:1723–1726.

Xia, R., T. Stangler, and J. J. Abramson. 2000. Skeletal muscle ryanodine receptor is a redox sensor with a well defined redox potential that is sensitive to channel modulators. *J. Biol. Chem*. 275:36556–36561.

Youdim, K. A., and S. G. Deans. 1999. Beneficial effects of thyme oil on age-related changes in the phospholipid C20 and C22 polyunsaturated fatty acid composition of various rat tissues. *Biochim. Biophys. Acta*. 1438:140–146.

Zhou, J., G. Brum, A. González, B. Launikonis, M. D. Stern, and E. Ríos. 2003. Ca^{2+} sparks and embers of mammalian muscle. Properties of the sources. *J. Gen. Physiol*. 122:95–114.

ZhuGe, R., K. E. Fogarty, R. A. Tuft, L. M. Lifshitz, K. Sayar, and J. V. Walsh, Jr. 2000. Dynamics of signaling between Ca^{2+} sparks and Ca^{2+}-activated K^+ channels studied with a novel image-based method for direct intracellular measurement of ryanodine receptor Ca^{2+} current. *J. Gen. Physiol*. 116:845–864.